THE CSU-RAMS CLOUD MICROPHYSICS MODULE:

GENERAL THEORY AND CODE DOCUMENTATION

PIOTR J. FLATAU, GREGORY J. TRIPOLI,
JOHANNES VERLINDE, WILLIAM R. COTTON

Colorado State University

DEPARTMENT OF ATMOSPHERIC SCIENCE

PAPER NO.
451

The CSU-RAMS Cloud Microphysics Module: General Theory and Code Documentation

Piotr J. Flatau, Gregory J. Tripoli*, Johannes Verlinde†
and William R. Cotton

Department of Atmospheric Science,
Colorado State University,
Fort Collins, Colorado 80523

September 1, 1989

Abstract

The new bulk microphysics scheme which was developed for use in the Colorado State University Regional Atmospheric Mesoscale Model (RAMS) is described. This scheme includes several unique concepts and should be easily transportable to other modeling systems. The new concepts include: Unifying treatment of different distributions (constant, gamma, Marshall-Palmer, and log-normal) which makes it possible to define the distribution-weighted properties in a simple and concise way. The introduction of a interaction scheme for water classes simplifies the description of all microphysical processes such as collection, vapor deposition, melting, riming, etc. A new method of finding exact and approximate integrals for collection processes is described. The scheme includes: cloud water, rain, pristine crystals, snow, graupel, and aggregates but the framework exist for additional classes such as hail. The introduction of two ice categories (pristine and snow) should improve prediction of ice properties and help properly parameterize other processes which are based on microphysics parameterization (such as radiative effects of cirrus clouds). A new set of prognostic equations for concentrations is included which will be used for modeling of such diversified situations as convective systems with imbedded stratiform regions or orographic systems. Beside this extensive theoretical development the new scheme is coded in standard FORTRAN 77, is parameter driven, and is written to function as a library module. This document includes a description of the code. It is optimized to run efficiently on vector machines.

*Current affiliation: University of Wisconsin, Dept. of Meteorology, Madison, WI 53715
†On special leave from the South African Weather Bureau

Contents

Aknowledgements

This research was supported by the National Science Foundation under grants ATM-8512480 and ATM-8814913, the Air Force Office of Scientific Research under contract AFOSR-88-0143 and the Army Research Office under contract DAAL03-86-K0175.

1 Introduction

One of the major objectives in science is to understand the basic processes to such an extend that man could modify or at least predict what is going to happen based on given input. In this document, our challenge is cloud and cloud systems. To fully understand these systems, mesoscale numerical models have been developed, simulating the physical processes involved. The processes in clouds do cover a broad range of typical sizes, and to formulate a numerical model of a complete system requires value judgements or compromises. The need to compromise becomes most obvious when one is faced with the task of formulating models of the microstructure of clouds (Cotton and Anthes, 1989). Yet, if we are to understand how the various processes interact to produce the final product, we have to develop some scheme to represent the smaller scale systems in the complete model.

Two types of schemes have been developed to simulate the microphysics involved in mixed phase clouds. The first type is to discretize the distribution of the different water categories into a small bins or elements (e.g. Young, 1974a). The different processes influencing the hydrometeors are then calculated, keeping track of the growth for all elements. This type of scheme requires huge memory allocation and is also very expensive on computer time. The second scheme is a bulk water type model, where it is assumed that the various water categories may be represented by continuous specified size distributions (e.g. Lin et al., 1983, Cotton et al., 1986). Bulk parameterizations are then developed for the various physical processes based on the assumed size distributions, transferring mass between the various categories of water classes. The second approach requires the formulation of simplifying assumptions, especially regarding the ice classes, but requires much less memory and make much more effective use of computer resources.

In this document a bulk microphysical parameterization scheme will be described. In the first part of the paper consideration will be given to the mathematical treatment of size distributions, and a generalized (for different distribution functions) scheme will be developed, which will make the implementation of various distribution functions in one model much easier. This scheme will allow the flexibility to change the assumed distribution by changing a single input variable. Then all the basic physics equations and concepts are given in part 2. Finally the bulk microphysical parameterization as is currently implemented in the CSU-RAMS model will be outlined, with

reference to the various subroutines and equations which are called in the module.

Part I

MATHEMATICAL CONSIDERATIONS

Although there is an apparent diversity of distributions that can be used to define the sizes of particles in atmospheric polidisperse media (clouds, fogs, aerosols), only a few types are observed to approximate the data well. These are: the generalized gamma distribution and its special cases (e.g. the exponential distribution), the normal distribution and its transformation (e.g. log-normal), the constant distribution, and the power law. The generalized or, as it is sometimes called in radiative transfer applications, *modified gamma* distribution defines as special cases the gamma, truncated gamma, exponential, Marshall-Palmer, Khrgian-Mazin, doubly truncated exponential, and the half-normal distributions. Even the normal and log-normal distributions can be linked to some of the mathematics arising in the generalized gamma distribution calculations. Here we try to derive a unified treatment of the size spectra and their moments for application in bulk microphysics parameterization schemes as is commonly used in atmospheric mesoscale models. We try to handle different size spectra with a few simple formulas which is general enough so as to encompass most of the size spectra and their moments in a mathematically similar expression. In a bulk microphysical scheme several water classes are usually considered, such as cloud particles, rain, aggregates, graupel, pristine ice, aerosols, and hail. In many parameterized rain models, specific reference is not made to the size distribution of the cloud droplets, but rain drops are usually considered to be distributed according to the exponential or log-normal distribution. The choice of a distribution function for a water class is by no means unique. The distribution which describes the averaged terminal velocity (or the raindroplet collection) the best may not be suitable to describe the radiative properties of the medium. This problem is rather fundamental nature. In most cases there is no deep underlying physical principle why the distribution should be of gamma, exponential, normal or any other type. The exponential distribution is motivated by the breakup-production balance, as well as ground-based and airborne measurements of raindrop spectra. Recently log-normal spectra were also found to fit observations pretty well (Feingold and Levin, 1986).

2 Size spectra and their moments

2.1 Basic concepts

Several formulas have been proposed to describe the distribution of the various water categories. The spectral density function $n(D)$ is defined such that $n(D)dD$ is the total number of particles with diameters between D and $D + dD$, per unit volume of air. Hence

$$N(D) = \int_0^D n(D)dD, \tag{2.1}$$

is the total concentration per unit volume of air of particles with diameters less than D. To describe a size spectrum we choose a suitable probability density function $f(D)$ defined over the interval (D_{min}, D_{max}). For most applications $D_{min} = 0$ and $D_{max} = \infty$, however, for generality, we will continue to use the interval (D_{min}, D_{max}). The form of the probability density function $f(D)$ has to meet a few simple criteria. It must be of an analytical form amenable to integration in a closed form so that the resulting mathematics is manageable. It must be a normalized function, and it must have only a few degrees of freedom, all of which should be possible to be diagnosed on the basis of bulk or spectral field measurements or model predictions.

The particle size distribution spectrum can then be represented by

$$n(D) = N_t f(D), \tag{2.2}$$

where N_t is the total concentration of particles per unit volume of air.

It is useful to develop a technique to define new probability density functions through a transformation of variables. From continuous distribution theory

$$f(D) = f(x)\frac{dx}{dD}, \tag{2.3}$$

if we can express the variable x as a arbitrary function of D, i.e. $x = h(D)$, and h is a arbitrary function. At this point we will also introduce a non-physical scaling diameter, D_n. This scaling diameter is used to present the spectral distribution function in a non-dimensional form. The scaling diameter will be related to physical quantities such as i.e. mean diameter of the distribution, but the relation will differ with spectral functions. In our generalized scheme it is convenient to use this scaling diameter rather than a specific physical quantity since this leads to simpler and general mathematics.

Averaged properties of the various water categories can be defined as

$$\overline{g} = \int_{D_{min}}^{D_{max}} g(D)n(D)dD. \tag{2.4}$$

The function g often exhibit a power law dependence, such that

$$g(D) = c_g D^{p_g} \tag{2.5}$$

where c_g and p_g are constants. The problem can then be reduced to finding the generalized moment of the distribution. The p^{th} moment of the distribution $f(D)$, defined over the interval (D_{min}, D_{max}) is

$$I(p, D_{min}, D_{max}) = \int_{D_{min}}^{D_{max}} D^p f(D)dD = D_n{}^p F(p, D_{min}, D_{max}). \tag{2.6}$$

The function F depends on the type of distribution assumed and the integration interval, and will be defined for various distributions in following sections. The advantage of using the scaling diameter can be seen here, the p^{th} power of the scaling diameter will be a result of the integration irrespective of the distribution assumed. Through this relation the scaling diameter can be defined in terms of measurable physical quantities, dependent on the assumed distribution.

Several moments are of special importance. The mean diameter and liquid water content are quantities frequently used in cloud modeling applications, while quantities such as the total surface area and the effective diameter are commonly used in radiative transfer models. The mean diameter of the distribution is as the first moment of the distribution and is defined as

$$\overline{D} = \int_{D_{min}}^{D_{max}} Dn(D)dD \Big/ \int_{D_{min}}^{D_{max}} n(D)dD. \tag{2.7}$$

The third moment of the distribution is proportional to water density for spherical particles, or the liquid or ice water content. The water content is defined as

$$l = \int_{D_{min}}^{D_{max}} m(D)n(D)dD, \tag{2.8}$$

where $m(D)$ is the mass of particle of diameter D. For spherical particles we have

$$m(D) = \frac{\pi}{6} D^3 \rho, \tag{2.9}$$

where ρ is density of particle. From (2.8) and (2.9)

$$l = \frac{\pi}{6}\rho N_t I(3, D_{min}, D_{max}) = \frac{\pi}{6}\rho N_t D_n^3 F(3, D_{min}, D_{max}). \tag{2.10}$$

This equation gives a relation between the water content l, the total concentration N_t, the type of distribution (represented by F) and the scaling diameter.

The total projected surface of particles is defined as

$$A_t = \int_{D_{min}}^{D_{max}} A(D)n(D)dD, \tag{2.11}$$

where A_t is total projected surface of the particles, $A(D)$ is the geometrical cross-section (or projected surface) of the particle of diameter D. For spherical particles $A(D) = \pi(D/2)^2$, for non-spherical particle $A(D)$ will depend on particular cross-section or, on the instantaneous orientation of the particle. Thus, in general the total surface will be a function of the second moment of the distribution. For spherical particles we have

$$A_t = N_t A(D_n) F(2, D_{min}, D_{max}) \tag{2.12}$$

The effective radius, often used in radiative transfer studies, is used to redefine the total surface, which is difficult to measure, in terms of the water content l, which is commonly measured. It is defined as

$$D_{\text{eff}} = \int_{D_{min}}^{D_{max}} n(D)D^3 dD \Big/ \int_{D_{min}}^{D_{max}} n(D)D^2 dD. \tag{2.13}$$

The diameter for which the distribution has a maximum is called the mode. The mode diameter can be obtained by differentiation of the distribution function f, setting it equal to zero and solving for the diameter.

2.2 The family of gamma distributions

A popular choice for the probability density function to describe sizes of atmospheric particles is the generalized gamma function. It is often used in radiative transfer, and is known there as the *modified gamma* distribution. It is defined as

$$f(x) = \frac{c}{s} x^{c\nu - 1} \exp\left(-x^c\right), \tag{2.14}$$

where c and ν define the shape of the distribution, and s is a normalization factor to ensure that integral of the distribution over the interval of definition is equal to 1. The *gamma* distribution can be obtained by setting $c = 1$ in this equation, and the *exponential* distribution may be obtained by setting $c = 1$ and $\nu = 1$. The *half-normal* distribution is another one of the family of gamma distributions, and it can be obtained by setting $c = 2$ and $\nu = \frac{1}{2}$.

The distribution function (2.14) can be transformed with the aid of eq (2.3). This leads to the form useful for atmospheric science applications. Let

$$x = \frac{D}{D_n}, \tag{2.15}$$

where D is diameter of particle and D_n is the *scaling* diameter. This transformation provides a non-dimensional parameter. After some simple algebra we obtain

$$f(D) = \frac{c}{s}\left(\frac{D}{D_n}\right)^{c\nu-1} \frac{1}{D_n} \exp\left[-\left(\frac{D}{D_n}\right)^{c}\right] \tag{2.16}$$

In addition to the previously defined parameters we have the *total concentration* N_t which relates the probability distribution function to the distribution spectrum (see 2.2). Thus there are four free parameters: D_n, c, ν, and N_t. One is easily measurable – the total concentration N_t. The shape parameters ν and c can also be measured but they are usually assumed on the basis of qualified intuition. The scaling diameter can be diagnosed from, say, water density (liquid or ice water content). If spectral data is available, both the scaling diameter and water density can be prognosed thus giving the opportunity to diagnose one of the shape parameters. Therefore we predict the free parameters from the *moments* of the distribution such as water content, scaling diameter, or total concentration.

A more general transformation $x = (D - D_0)/D_n$ is possible. Here D_0 allows for the shift of D-axis, but we will set $D_0 = 0$ throughout this section.

2.2.1 Truncated general gamma distribution

The truncated gamma distribution will be the most general form of the modified gamma distribution we will deal with. On the basis of some additional hypotheses we may assume that smaller or larger diameters of the spectrum are not observed or not needed in the calculations. The size

spectrum may be, for example, the generalized gamma distribution, but with one, or both ends of the spectrum truncated. Although this is conceptually simple, the concept may sometimes lead to awkward mathematics. In the case of the gamma distribution and its relatives moments of the distribution are a function of the incomplete gamma functions $\gamma(x,y)$ and $\Gamma(x,y)$, instead of the complete gamma function $\Gamma(x)$ (Appendices A and B).

We will define the truncated gamma distribution as equation (2.16) defined over the interval (D_{min}, D_{max}). The parameter s can then be derived from the requirement that the distribution has to be normalized over the interval of definition. Namely

$$\int_{D_{min}}^{D_{max}} f_{tmg}(D) = 1, \tag{2.17}$$

where the subscript *tmg* stands for *truncated modified gamma.* Substituting from equation (2.16) and performing the integration gives the desired expression for s

$$s_{tmg}(D_{min}, D_{max}) = \gamma\left[\nu, (D_{max}/D_n)^c\right] - \gamma\left[\nu, (D_{min}/D_n)^c\right]. \tag{2.18}$$

The moments of the truncated modified gamma distribution are now defined as

$$I_{tmg}(p) = \int_{D_{min}}^{D_{max}} D^p f(D) dD = D_n^p F_{tmg}(p), \tag{2.19}$$

where

$$F_{tmg}(p) = \frac{1}{s}\left[\gamma\left(\nu + p/c, (D_{max}/D_n)^c\right) - \gamma\left(\nu + p/c, (D_{min}/D_n)^c\right)\right]. \tag{2.20}$$

2.2.2 Generalized gamma distribution

In most applications in atmospheric science the interval over which the distribution is defined is taken as $(0, \infty)$. This leads to simplified mathematics where the function F can be expressed in terms of the complete gamma function $\Gamma(x)$ (Appendix A). The parameter s will be $\Gamma(\nu)$ for this definition, so that the form for the general modified gamma distribution will be

$$f_{mg}(D) = \frac{c}{\Gamma(\nu)}\left(\frac{D}{D_n}\right)^{c\nu-1}\frac{1}{D_n}\exp\left[-\left(\frac{D}{D_n}\right)^c\right], \tag{2.21}$$

where the subscript *mg* refers to modified gamma. This form of the distribution is popular in radiative transfer applications.

The moments of the modified gamma distribution are then defined as

$$I_{mg}(p) = \int_0^\infty D^p f_{mg}(D) dD = D_n^p F_{mg}(p), \tag{2.22}$$

where

$$F_{mg}(p) = \frac{\Gamma(\nu + p/c)}{\Gamma(\nu)}. \tag{2.23}$$

From (2.22) we can attempt to diagnose the free parameters of the distribution. First let us consider the relationship between the scaling diameter D_n and the *mean diameter*, *effective diameter*, and *modal diameter* of the distribution, where we assume the interval of integration to be $(0, \infty)$. From the definition (2.7) of the mean diameter we have

$$D_{mean} = \frac{F_{mg}(1)}{F_{mg}(0)} D_n = \frac{\Gamma(\nu + 1/c)}{\Gamma(\nu)} D_n$$

where the last result follows from (2.23), i.e. $F(1) = \Gamma(\nu + 1/c)/\Gamma(\nu)$ and $F(0) = 1$. The effective diameter D_{eff} is defined by (2.13) which gives

$$D_{\text{eff}} = \frac{F_{mg}(3)}{F_{mg}(2)} D_n = \frac{\Gamma(\nu + 3/c)}{\Gamma(\nu + 2/c)} D_n.$$

The mode diameter D_{mode}, for which the distribution has maximum, can be obtained by differentiation of the generalized gamma function (2.16). This gives

$$D_{mode} = \left(\nu - \frac{1}{c}\right)^{1/c} D_n.$$

If one of the parameters D_{mode}, D_{mean}, or D_{eff} is somehow predicted or can be measured, we can estimate the scaling diameter D_n. Another way to obtain it is from a higher moment, like liquid water content or reflectivity.

It was shown (2.10) that for spherical particles the liquid water can be determined from the relation $l = \pi/6 N_t D_n^3 \rho F(3)$. Then, for the modified gamma distribution we get

$$l = \frac{\pi}{6} N_t D_n^3 \rho \frac{\Gamma(\nu + 3/c)}{\Gamma(\nu)} \tag{2.27}$$

In some applications we need moments that are calculated up to or from a specific diameter D_{cut}, or over the intervals $(0, D_{cut})$ and (D_{cut}, ∞). In this case the function F is give by

$$F_{mg}(p, 0, D_{cut}) = \frac{\gamma\left[\nu + p/c, (D_{cut}/D_n)^c\right]}{\Gamma(\nu)} \tag{2.28}$$

and

$$F_{mg}(p, D_{cut}, \infty) = \frac{\Gamma\left[\nu + p/c, (D_{cut}/D_n)^c\right]}{\Gamma(\nu)} \tag{2.29}$$

Here we need to distinguish these functional forms from that of the truncated gamma distribution over the interval $(0, D_{cut})$ and (D_{cut}, ∞). These are integrations over a part of the full normalized distribution, whereas for the truncated distributions the distribution is normalized over that part of the spectrum.

Gamma distribution

The gamma distribution can be obtained from the modified gamma distribution by letting $c = 1$. Since the change in the mathematics is minimal, we will simply give the probability density function for reference, and the functional form for F. The probability density function is given by

$$f_{gam}(D) = \frac{1}{\Gamma(\nu)} \left(\frac{D}{D_n}\right)^{\nu-1} \frac{1}{D_n} \exp\left(-\frac{D}{D_n}\right), \tag{2.30}$$

where the subscript *gam* refers to gamma. The functional form of F is given by

$$F_{gam}(p) = \frac{\Gamma(\nu + p)}{\Gamma(\nu)}. \tag{2.31}$$

For the rest of the equations the reader is referred to the previous section.

Exponential distribution

An important case of the generalized gamma distribution is that of purely exponential dependence when we set $c = 1$ and $\nu = 1$. This is known in atmospheric science field as the *Marshall-Palmer*

(MP) type size spectrum and the *exponential* probability function in statistics. All the formulas are already derived in the previous section, but we repeat some of them here for completeness. For $c = 1$ and $\nu = 1$ we get

$$f_{\mathrm{MP}}(D) = \frac{1}{D_n} \exp\left(-\frac{D}{D_n}\right).$$

where D_n again is the scaling diameter. A related quantity is called slope and is defined as (Manton and Cotton, 1977)

$$\Lambda = \frac{1}{D_n}.$$

If D_n increases, the distribution is becoming flatter (less steep), and slope Λ decreases. Therefore, for large D_n the size spectrum becomes uniform. For the full exponential distribution ($D \in (0, \infty)$) the moments are again defined as

$$I_{\mathrm{MP}}(p) = \int_0^\infty D^p f(D) dD = D_n^p F_{\mathrm{MP}}(p). \tag{2.34}$$

where, in this case, the function F is defined by

$$F_{\mathrm{MP}}(p) = \Gamma(p+1). \tag{2.35}$$

The exponential distribution has a maximum (mode diameter of the distribution) at $D = 0$, as can be predicted from (2.32). The relationships between the scaling diameter and the mean and the effective diameters are then given by

$$D_{mean} = D_n, \quad D_{mode} = 0, \quad D_{\mathrm{eff}} = 3D_n. \tag{2.36}$$

Thus, the scaling diameter is equal to the mean diameter if the exponential distribution is assumed. For completeness we will once again write down the functional forms for integration over the intervals $(0, D_{cut})$ and (D_{cut}, ∞) F:

$$F_{\mathrm{MP}}(p, 0, D_{cut}) = \gamma(p+1, \frac{D_{cut}}{D_n}),$$

and

$$F_{\mathrm{MP}}(p, D_{cut}, \infty) = \Gamma(p+1, \frac{D_{cut}}{D_n}). \tag{2.38}$$

2.2.5 Half-normal distribution

Another special case of the generalized gamma probability density function is the *half-normal* distribution. The half-normal distribution is obtained from the generalized gamma distribution by setting $c = 2$ and $\nu = 1/2$. Of course all of the previous results (moments, mean, effective, and mode diameter, etc) apply. This distribution is a middle-step for the derivation of the normal and log-normal spectrum and we will provide the form of probability density function for future reference. Let $c = 2$ and $\nu = 1/2$ in (2.16), and then also notice that $\Gamma(1/2) = \sqrt{\pi}$. This gives

$$f_{hn}(D) = \frac{2}{\sqrt{\pi}} \frac{1}{D_n} \exp\left[-\left(\frac{D}{D_n}\right)^2\right] \tag{2.39}$$

which is known as the *half-normal* distribution (*hn* stands for half-normal). The *half* comes from the fact that we deal with positive diameters D, i.e D defined on $(0, \infty)$.

In both the exponential and the half-normal distributions the *shape* parameters c and ν have been fixed, thus there will be less degrees of freedom. Only the scaling diameter D_n and total concentration N_t can be varied. This, however, is not as restrictive as it appears at the first glance, since the choice of a particular distribution is more or less arbitrary in any case.

2.3 Normal and log-normal distributions

2.3.1 Normal distribution

The normal distribution has the same mathematical structure as the half-normal distribution, but it is defined for $D \in (-\infty, \infty)$. The probability density function is given by

$$f_{nor}(D) = \frac{1}{\sqrt{2\pi}} \frac{1}{D_n} \exp\left[-\frac{1}{2}\left(\frac{D}{D_n}\right)^2\right]. \tag{2.40}$$

The normal distribution has no real applications in the field of microphysics, since it predicts no-zero probabilities for negative diameters ($D < 0$). It can, however, suitably be *transformed*, such that diameters in the range $(-\infty, \infty)$ are mapped to $(0, \infty)$. This is the case of the *log-normal* distribution, which will be defined in the next section.

2.3.2 Log-normal distribution

The log-normal distribution is a transformation of the *normal* probability density function. Consider the standard mathematical form of the normal distribution (discussed in the previous section) of a variable x

$$f_{nor}(x) = \frac{1}{(2\pi)^{1/2}} \exp\left(-\frac{1}{2}x^2\right) \tag{2.41}$$

We will introduce the transformation

$$x = \frac{1}{\sigma} \ln\left(\frac{D}{D_n}\right), \quad x \in (-\infty, \infty), \tag{2.42}$$

where D_n and σ are parameters. This transformation maps $x \in (-\infty, \infty)$ into $D \in (0, \infty)$. From (2.3) we then obtain

$$f_{log}(D) = f_{nor}(x)\frac{dx}{dD} = \frac{1}{\sqrt{2\pi}\sigma D} \exp\left[-\left(\frac{\ln(D/D_n)}{\sqrt{2}\sigma}\right)^2\right], \quad D \in (0, \infty). \tag{2.43}$$

In this distribution the *logarithm* of the diameter is normally distributed. To find the mean of the distribution $f(x)$ we multiply (2.41) by u and integrate over $(-\infty, \infty)$. The result will be 0, since $f(x)$ is symmetric about 0. Then from (2.42) we get

$$\overline{\ln(D)} = \ln D_n.$$

where

$$\overline{\ln(D)} = \int_0^\infty \ln(D) f_{log}(D) dD.$$

Similarly, it can be shown that

$$\sigma^2 = \overline{(\ln \frac{D}{D_n})^2}. \tag{2.46}$$

The moments of f_{log} are

$$I_{log}(p) = \int_0^\infty D^p f_{log}(D) dD = N_t D_n^p F_{log}(p), \tag{2.47}$$

where

$$F_{log} = \exp\left(\frac{\sigma^2 p^2}{2}\right) \tag{2.48}$$

The mean diameter is

$$D_{mean} = \frac{F_{log}(1)}{F_{log}(0)} D_n = \exp\left(\frac{\sigma^2}{2}\right) D_n. \tag{2.49}$$

The effective diameter is

$$D_{\text{eff}} = \exp\left(\frac{9}{5}\sigma^2\right). \tag{2.50}$$

The water content is

$$q = \frac{\pi}{6} N_t D_n^3 \rho \exp\left(\frac{9}{2}\sigma^2\right)$$

2.4 Constant distribution

The probability density function of the constant or monodisperse distribution is defined as

$$f_{con}(D) = N_t \delta(D - D_n)$$

The function $\delta(D - D_n)$ is the Dirac's delta function which will prove useful for definitions of distribution-averaged quantities. This function is 1 for $D = D_n$ and 0 otherwise. The moments are simple, and are given by

$$I_{con}(p) = \int_0^\infty D^p f_c(D) dD = D_n^p.$$

Thus

$$F_{con}(p) = 1$$

for all values of p.

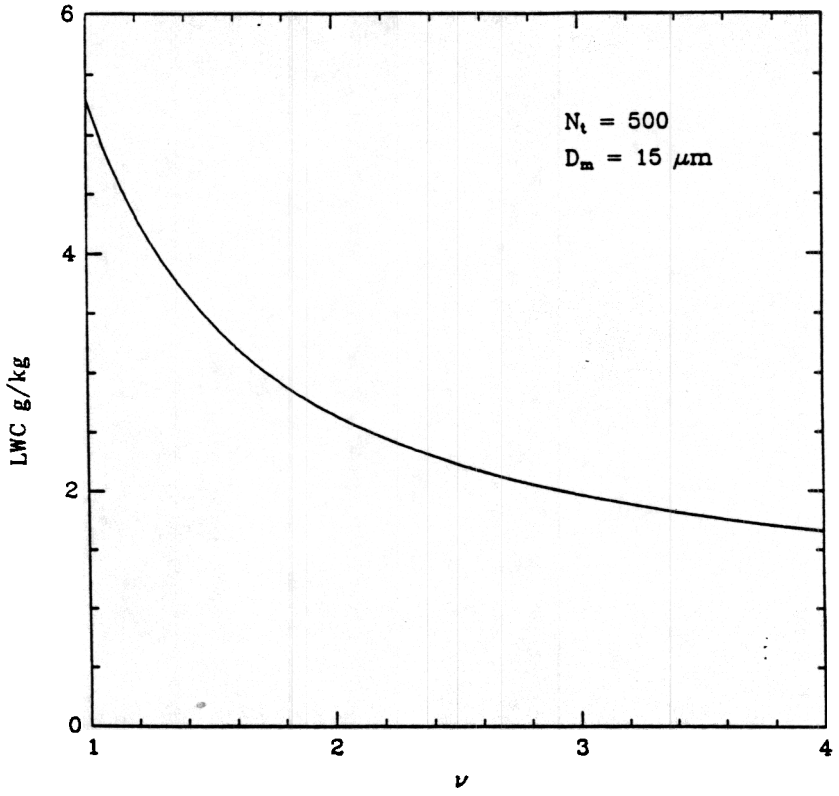

Figure 2: Liquid water dependence on shape parameter ν. This is for a modified gamma distribution ($c = 1$) with mean diameter 15 μm and total concentration 500 particles per cm^3.

Relationships between parameters and other moments

In atmospheric science applications it is often assumed that $c = 1$, which leave three free parameters in the gamma type distributions. It is sensible to choose three parameters which are measurable or are based on some physical intuition to characterize the size spectrum. The simplest one is (N_t, ν, D_n). Another possibility is the triplet (N_t, D_{mode}, l). Many devices can measure water content and total number directly, and while ν or D_{mode} is obtainable from the size spectra. Other choices could be motivated by more theoretical reasoning. In radiative transfer the total extinction of light by the particle is related to the total surface of particles A_t. Thus, for theoretical purposes, it is of interest to keep the total area the same and vary other parameters to study the sensitivity of the radiative transfer of light to choices of those parameters, or thus for different clouds. The triplet (N_t, A_t, l) would be advisable in such case. The total projected area can actually be estimated from PMS probes (2C and 2D probes) (e.g. Gordon and Marwitz, 1984). Other choices are also possible.

A word of warning is in place here. The choice of a three-parameter (or in that matter four-parameter) distribution is quite restrictive as it forces us to define all physics in terms of a finite number of moments. For example N_t, D_{mode} and l defines the gamma distribution completely. Then the standard deviation or spread of the distribution cannot be controlled without difficulty.

(2.5) shows two distributions for different ν but the same modal diameter D_{mode} and total concentration N_t. The solid line is for $\nu = 1.5$ and the dashed line is for $\nu = 3$. The $\nu = 1.5$ case contains more large droplets, thus leading to much larger liquid water content. Fig. (2.5) shows the dependence of water content l on the parameter ν defined by (2.21). It can be seen that small values of ν indicate large values of water content. Thus, we can see the sensitivity of the physical moments to the parameters of the distribution.

We will refer to the set (N_t, ν, D_n, c), $c = 1$, as the set of base parameters. We will now proceed to derive relationships between the base parameters and the more common measurable parameters. From (2.26) we have $D_n = D_{mode}/(\nu - 1/c)^{1/c}$, the relationship between D_{mode} and D_n. If we substitute this into (2.27) we get

$$(\nu/c - 1)^{3/c} \frac{\Gamma(\nu)}{\Gamma(\nu + 3/c)} = \frac{N_t \pi \rho_w D_{\text{mode}}^{3/c}}{6l} \tag{2.55}$$

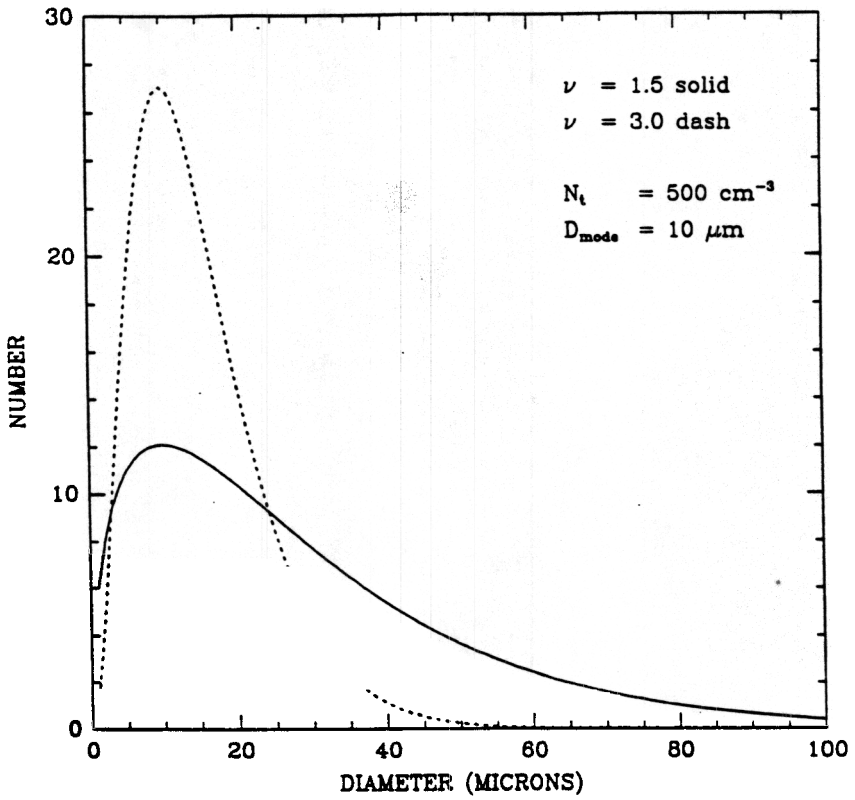

Figure 1: Droplet size distribution for modified gamma distribution, $c = 1$, with same modal diameter (15 μm) and total concentration (500 per cm^3), but with *a*) $\nu = 1.5$, *b*) $\nu = 3$.

This nonlinear equation may be solved for ν. Thus, given observations of the modal diameter and the water content, the base parameters of the distribution can be determined. Similarly, if the liquid water content and the total projected area are known, then from equations (2.12) and (2.27) the following relationship can be derived

$$\frac{\Gamma(\nu+2/c)^3}{\Gamma(\nu+3/c)^2\Gamma(\nu)} = \frac{A_t^3\rho_w^2}{36\pi N_t l^2}. \tag{2.56}$$

Once ν is defined from (2.56) the D_n can be subsequently obtained from (2.12). With other measured quantities similar relationships can be derived. Thus, it is feasible, albeit not simple (equations 2.27 and 2.56 are non-linear), to extract the basic parameters from a measured data set. In the following sections we will then develop the parameterization scheme in terms of the basic parameters.

3 Summary

In this section we have developed a general mathematical structure that will be used throughout the rest of the document. A summary of the notations are given in Table 1 and Table 2. In Table 3 the general forms of the truncated distributions are given, with the function G_1 representing integration from 0 to a cut-off diameter D_{cut} and G_2 integration from D_{cut} to ∞. It was shown that for most of the distributions the moments may be expressed in the same mathematical form by Equation 2.6, where only the function F change for the different distributions. If it is assumed that properties of the various water classes such as mass or vertical velocity can be written in the form of power laws, then the bulk parameterization scheme can be developed in a general form in terms of F. This will allow that any distribution may be assumed of any of the water classes, without duplication and hardwiring of code. We now have the mathematical tools needed to develop the parameterization scheme.

Distribution	Symbol	D_{min}	D_{max}	c	ν
Modified gamma	*mg*	0	∞	c	ν
Gamma	*gam*	0	∞	1	ν
Exponential	*MP*	0	∞	1	1
Half-normal	*hn*	0	∞	2	1/2
Normal	*nor*	$-\infty$	∞	-	-
Log-normal	*log*	0	∞	-	-

Table 1: Summary of the size distributions and the shape parameters c and ν.

Name	Modified gamma	Exponential	Log-normal
$F(p)$	$\Gamma(\nu+p/c)/\Gamma(\nu)$	$\Gamma(p+1)$	$\exp(\sigma^2 p^2/2)$
D_{mean}	$\Gamma(\nu+1/c)/\Gamma(\nu)D_n$	D_n	$\exp(\sigma^2/2)D_n$
D_{eff}	$\Gamma(\nu+3/c)/\Gamma(\nu+2/c)D_n$	$3D_n$	$\exp(5\sigma^2/2)D_n$
D_{mode}	$(\nu-1/c)^{1/c}D_n$	0	$D_n\exp(-\sigma^2)$
Water content q	$\pi/6N_tD_n^3\rho\Gamma(\nu+3/c)/\Gamma(\nu)$	$\pi/6N_tD_n^3\rho\Gamma(4)$	$\pi/6N_tD_n^3\rho\exp(9\sigma^2/2)$

Table 2: General functional form and special moments for the more generally used size distributions

Distribution	$G_1(p, D_{cut})$	$G_2(p, D_{cut})$
Constant	0 for $D_{cut} < D_n$ 1 for $D_{cut} > D_n$	1 for $D_{cut} < D_n$ 0 for $D_{cut} > D_n$
gamma	$\frac{\gamma(\nu+p+1, a\frac{D_{cut}}{D_n})}{a^p\Gamma(\nu+1)}$	$\frac{\Gamma(\nu+p+1, a\frac{D_{cut}}{D_n})}{a^p\Gamma(\nu+1)}$
M-P	$\gamma(p+1, \frac{D_{cut}}{D_n})$	$\Gamma(p+1, \frac{D_{cut}}{D_n})$
Truncated M-P	$\frac{1}{s}\left[\gamma(p+1, \frac{D_{cut}}{D_{ne}}) - \gamma(p+1, \frac{D_{min}}{D_{ne}})\right]$	$\frac{1}{s}\left[\Gamma(p+1, \frac{D_{cut}}{D_{ne}}) - \gamma(p+1, \frac{D_{min}}{D_{ne}})\right]$

Table 3: Truncated distributions and their general functional forms. The function G_1 represents integration from 0 to a cut-off diameter D_{cut} and G_2 integration from D_{cut} to ∞.

Part II

CLOUD MICROPHYSICAL PROCESSES A REVIEW OF FUNDAMENTAL PRINCIPLES AND PARAMETERIZATIONS

The microphysical processes in a cloud are those physical processes leading to the formation and growth of the particles. These particle can be liquid, or ice, or a combination of both, and may have a regular or irregular shape. They are generally classified in several categories as cloud droplets (c), rain drops (r), ice crystals (i), snow crystals (s) or aggregates (a), and graupel or hail (g). Depending on the application, all or only some of these categories may be selected. Each category may grow independently from vapor and self collection, or may interact with the other categories through collision and coalescence. It is hoped that this general parameterized scheme may provide a measure of comparison between schemes implemented on various models. The notation used in this section, and the rest of this document, will be to use no subscript when general single category equations are described (like the vapor deposition equation), and to use the subscripts x and y when we are dealing with general multiple category interactions (like riming growth). When dealing in specific applications, the subscript(s) for the specific category(ies) will be used.

4 Cloud Physics

The basic equations governing the physical processes leading to the formation of precipitation particles in clouds will be discussed in this section. It will first be established that mass, density and terminal velocity may be expressed in the form of a power law relationship with diameter, and then some relations between mixing ratio, total concentration and diameter will be developed. Based on these relationships all the physical processes are then described. The development of all the equations follow the CSU-RAMS formulations to a large extent, although thought also is given to alternative ideas.

4.1 Power law relationships

Theoretical and/or empirically determined power laws of the form

$$g(D) = c_g D^{p_g}$$

have been proposed for cloud microphysical particle characteristics such as density, mass and terminal velocity. In this formulation D is the particle diameter.

4.1.1 Density-diameter dependence

The density of a particle is denoted as ρ. In general this may be expressed in the form of a power law.

$$\rho = c_\rho D^{p_\rho}$$

For all the liquid water categories the density is constant, i.e. $p_{\rho r} = 0$. This will be true for some of the ice phase particles, such as hail, however, for most of the ice phase particles the more general formulation is needed. These formulations are generally empirically determined. Pruppacher and Klett (1978) , based on results from Heymsfield (1972) , and Ryan et al. (1976) have reported on relationships for single ice crystals (pristine ice), while Passarelli and Srivastava (1979) , based on data from Magono and Kakamura (1965) , have fitted a power law dependence of density to diameter for aggregates.

4.1.2 Mass-diameter dependence

The mass of a individual particle depends on its shape and density and, therefore, may be a complicated function of diameter. However, we will again assume that it can be expressed in the form of a simple power law as

$$m(D) = c_m D^{p_m}$$

- For spherical particles of diameter D this relationship may be derived analytically:

$$m(D) = \frac{4}{3}\pi\left(\frac{D}{2}\right)^3 \rho = \frac{\pi}{6} D^3 \rho.$$

Combining (4.4) and (4.2) we get

$$m(D) = \frac{\pi}{6} c_\rho D^{3+p_\rho},$$

From equation (4.3) we notice that

$$c_m = \frac{\pi}{6} c_\rho,\ p_m = 3 + p_\rho.$$

- For ice phase particles empirical relationships derived from laboratory experiments reported by Locatelli and Hobbs (1974) can be used. For example, snow crystals have

$$D = x_1 m^p \tag{4.7}$$

or, by simple algebra,

$$m = c_m D^{p_m} \tag{4.8}$$

where

$$c_m = \left(\frac{1}{x_1}\right)^{1/p},\ p_m = \frac{1}{p}$$

4.1.3 Terminal velocity

The terminal velocity of water droplets or ice crystals is derived in this section. For spherical particles theoretical formulations can be derived, but for more complex shapes such as hexagonal ice crystals empirical formulas are used. We will denote the terminal velocity by v. With the variety of formulations, most can be summarized by

$$v = c_v D^{p_v}$$

Theoretically terminal velocities can be derived by solving the Navier-Stokes equations with appropriate boundary conditions. In the derivation a non-dimensional quantity, the Reynolds number, is used. The Reynolds number is a measure of the relative balance (importance) of non-linear advection term to viscous acceleration in the steady state Navier-Stokes equation and is defined by

$$Re = v\frac{D}{\nu} \tag{4.11}$$

where ν is the kinematic viscosity.

For small Reynolds numbers the non-linear terms in the Navier-Stokes equations can be neglected. It can then be solved analytically for simple geometries to give particularly simple formulas. Many cloud particles indeed have Reynolds numbers smaller than unity. But even in the small Reynolds number limit one has to use numerical solutions for more complex shapes.

In the large Reynolds number (> 1) limit, things quickly become complicated. As Re increases, the flow becomes more complicated as the non-linear term becomes more important. An additional complication is the change of shape for larger drops. In the large Reynolds number limit solutions are virtually always obtained with the help of computer. It is interesting to note that only very idealized solutions exist for ice crystals with large Reynolds numbers. In this case it is better to resort to experimental formulations.

- Spherical particles

  For a spherical drop falling at its terminal velocity in air, the equation of motion reduces to the balance of gravity and viscous drag forces

$$\frac{\pi}{6}D^3\rho g = \frac{1}{2}\pi\left(\frac{D}{2}\right)^2\rho_0 v^2 C_D$$

  where C_D is the drag coefficient. This can be rewritten as

$$v = \left(\frac{4}{3}\frac{\rho g}{\rho_0 C_D}\right)^{1/2} D^{1/2}. \tag{4.13}$$

  If the density depends on diameter as in (4.2) we can write (4.13) as

$$v = \left(\frac{4}{3}\frac{g c_\rho}{\rho_0 C_D}\right)^{1/2} D^{(1+p_\rho)/2} \tag{4.14}$$

  thus

$$c_v = \left(\frac{4}{3}\frac{g c_\rho}{\rho_0 C_D}\right)^{1/2},\ p_v = \frac{1+p_\rho}{2}$$

For small, spherical droplets one can show that the drag coefficient is (Stoke's solution)

$$C_D = \frac{24}{Re}.$$

This equation, the definition of the Reynolds number (4.11) and the relationship between kinematic and dynamic viscosity (4.17)

$$\nu_d = \frac{\mu_d}{\rho_d}$$

substituted into (4.13) give the following simple quadratic dependence for the terminal velocity

$$v = \frac{1}{18}\frac{g\rho}{\mu}D^2 = c_v D^2 \tag{4.18}$$

This quadratic dependence of fall velocities on size is called Stoke's Law and applies to cloud droplets up to about 80 μm diameter (Rogers, 1979, p. 91).

- Non-spherical Particles.

  For non-spherical liquid drops the radius of a sphere of equal volume is normally used, and C_D is adjusted accordingly. Clearly, the problem of using (4.14) to predict v is centered around the determination of C_D, which for a rigid body, is a function of the Reynolds number. As was discussed, this may quickly become quite complex, therefore it is eassier to resort to empirical formulations.

- Empirical formulas.

  For ice crystals, which are of complex shape, porous, and of varying density, many empirical formulas have been proposed. Most are of the type given by (4.10). For example, results reported by Hobbs (91972) and Locatelli and Hobbs (1974) can by used. In using these laboratory results conducted at sea level, care should be taken to apply the Foote and du Toit (1969) , correction into account for the decreased resistance of air at lower pressures.

See for example Table 8 for the relationships used in the CSU-RAMS model.

4.2 Mass-weighted terminal velocity

The mass-weighted terminal velocity is given by

$$\overline{v} = \frac{1}{\overline{r}\rho_0} \int_0^\infty m(D)v(D)n(D)dD \tag{4.19}$$

which, after integration gives

$$\overline{v} = \frac{1}{\overline{r}\rho_0} v(D_n)m(D_n)N_t F(p_m + p_v) \tag{4.20}$$

where p_m and p_v are the power coefficients arising in formulas (4.3) and (4.10), and $\overline{r}$ is the weighted average mixing ratio defined by

$$\overline{r} = \frac{1}{\rho_0} \int_0^\infty m(D)n(D)dD. \tag{4.21}$$

Using the mass-diameter relationship (4.3), integration of (4.21) gives

$$\overline{r} = \frac{1}{\rho_0} N_t m(D_n)F(p_m) \tag{4.22}$$

Substitution of this in (4.20) gives the desired simple formulation of the mass-weighted average terminal velocity

$$\overline{v} = \frac{F(p_v + p_m)}{F(p_m)} v(D_n)$$

4.3 Total concentration

The mixing ratio is generally the prognostic variable and the total concentration can then be obtained diagnostically from (4.22) as

$$N_t = \frac{\rho_0}{m(D_n)} \frac{1}{F(p_m)} \overline{r}.$$

Otherwise explicit predictive equations for N_t of a particular species is formulated.

4.4 Diameter derived from concentration and mixing ratio

If both the concentration N_t and the mixing ratio $\overline{r}_x$ are derived from prognostic equations we can further manipulate (4.22) to get

k	C	Location	Reference
0.7	100	Maritime air	Twomey and Wojciechowski, 1969
0.5	600	Continental air	Twomey and Wojciechowski, 1969
0.4	2000	Australia (Con)	Twomey, 1959
0.3	125	Australia (Mar)	Twomey, 1959
0.9	3500	Buffalo, N.Y.	Kochmond, 1965
0.46	53	Hilo, Hawaii	Jiusto, 1967
0.63	105	Hawaii (Con)	Jiusto, 1967
0.64	3990	High $(S-1)$	Alofs and Lui, 1981
3.85	6.62×10^7	High $(S-1)$	Alofs and Lui, 1981

Table 4: Summary of values of constants for CCN counts reported in literature for different locations and airmasses.

$$D_n = \left(\frac{\rho_0}{c_m}\frac{\overline{r}}{N_t}\right)^{\frac{1}{p_m}} \tag{4.25}$$

4.5 Nucleation

All particles in a cloud have to develop in some way or another either from nucleated cloud water or nucleated ice water. These processes and their mathematical description are therefore very important to any cloud model.

4.5.1 Nucleation of cloud water

The concentration of cloud condensation nuclei increases with increasing supersaturation. This can be expressed in the form

$$N_{CCN} = C(S_v - 1)^k \tag{4.26}$$

where k and C are approximately constant and dependent on the type of airmass (Pruppacher and Klett, 1978). S_v is the saturation value with respect to water. A variety of values have been reported in the literature for these constants (see Table 4).

Twomey (1959) has obtained approximate expressions for upper bounds of $(S_v - 1)$ and N in rising air parcels. After deducing $(S_v - 1)_{max}$, the corresponding value of N_{max} can be deduced from (4.26). This expression for $(S_v - 1)_{max}$ takes on the form

$$(S_v - 1)_{max} = C^{-1/(k+2)} \left[\frac{Aw^{3/2}}{kB(k/2, 3/2)} \right]^{1/(k+2)}$$

where w [cm s^{-1}] is the vertical velocity, k and C are the same as in (4.26), $B(x,y)$ is the Beta function, and A is a constant, given by Pruppacher and Klett (1978) , as 6.9×10^{-2}.

4.5.2 Primary nucleation of ice

There are four processes through which ice may be nucleated in the atmosphere: deposition nucleation, immersion freezing, condensation freezing and contact nucleation. The amount of ice nuclei (IN) active in each process, and its dependence on temperature and supersaturation is not well understood. The most common approach is to approximate the amount of ice crystals at a given degree of supercooling with the Fletcher curve (Fletcher, 1962)

$$N_i = N_0 \exp(aT_{sup}) \tag{4.28}$$

where $N_0 = 10^{-5} l^{-1}$ and $a = 0.6(^\circ C)^{-1}$ are constants and T_{sup} is the degree of supercooling.
tion 4.28 was derived from the average spectra of ice nuclei measurements. Those measurements, however, were at water saturation and did not sustain a cloud long enough to measure contact nucleation.
Cotton et al. (1986) , generalized the Fletcher equation to include a supersaturation dependence using equations developed by Huffman and Vali (1973) . The deposition/condensation freezing is then modeled by

$$N_i = N_0 B \left[\frac{(S_i - 1)}{(S_0 - 1)} \right]^b \exp(aT_{sup}),$$

where b and B are constants and $(S_0 - 1)$ represents the percent ice supersaturation of a water saturated cloud. Cotton et al. (1986) chose $b = 4.5$ and $B = 3.15$ m^{-3}
Stepanov (1986) , have reported on ice nuclei concentration values as a function of temperature and supersaturation with respect to ice. D. Rogers (personal communication) fit a bi-linear equation to the data of the form

$$N_i = 0.956 + 0.12T - (0.316 + 0.036T)(S_i - 1)$$

which is valid for $T < -8°C$. We plan to implement (4.30) and examine the sensitivity of the model to the two formulations. Clearly Equation (4.30) is based on a consistent set of observations, whereas Equation (4.29) is based on a piecing together of independent observations and averages of observations from different ice nuclei counters.

Based on Young (1974a,b) contact nucleation is treated by considering Brownian diffusion, thermophoresis and diffusiophoresis processes. Cotton et al. (1986) scaled Young's equations to come up with the following expressions: For Brownian diffusion nucleation

$$N_B = m_{i0} F_1 D_{ar} \tag{4.31}$$

for thermophoretic nucleation

$$N_{Th} = \frac{1}{\rho_0} m_{i0} F_1 F_2 f_t \tag{4.32}$$

and for diffusiophoretic nucleation

$$N_{Di} = \frac{1}{\rho_0} m_{i0} F_1 D_v \frac{[e_v - e(R_c)]}{p} \tag{4.33}$$

where m_{i0} corresponds to the initial mass of the nucleated ice crystal, D_{ar} is the aerosol diffusivity, and e_v and $e(R_c)$ are the vapor pressures at infinity and the droplet surface. F_1, F_2 and f_t are defined by the following expressions.

$$F_1 = \frac{1}{\rho_0} 4\pi R_c N_c N_a$$

$$F_2 = \frac{k}{p}(T - T_c)$$

$$f_t = \frac{0.4[1 + 1.45K_n + 0.4K_n \exp(-1/K_n)](k + 2.5K_n k_a)}{(1 + 3K_n)(2k + 5k_a K_n + k_a)} \tag{4.36}$$

where R_c is the cloud droplet radius, N_c is the cloud droplet concentration, N_a is the concentration of active contact nuclei, k is the thermal conductivity, k_a is the aerosol thermal conductivity, K_n is the Knudsen number, T_c is the cloud droplet temperature and T the environment temperature while p is the environmental pressure. The Knudsen number K_n is defined as

$$K_n = \frac{7.37T}{288pR_a} \tag{4.37}$$

where R_a is an assumed aerosol radius. The concentration of active contact nuclei N_a is given by

$$N_a = N_{a0}(270.16 - T_c)^{1.3} \tag{4.38}$$

where T_c is the cloud droplet temperature and $N_{a0} = 2 \times 10^{-1}$ cm^{-3}. The aerosol diffusivity D_{ar} is defined by

$$D_{ar} = \frac{7.32 \times 10^{-18} T_c}{R_a \mu}(1 + K_n) \tag{4.39}$$

The total number of crystals nucleated by contact nucleation is then given by the sum of the three process.

4.5.3 Secondary nucleation of ice

Gordon and Marwitz (1981) , have developed a parameterization for the Hallet-Mossop ice multiplication theory. They have two basic models

Approximately 350 ice splinters are produced for every milligram of rime accreted onto each graupel particle at -5°C (Hallet and Mossop, 1974). This mechanism was formulated using

$$P_p(I) = 3.5 \times 10^5 \text{g}^{-1} \frac{dm}{dt}\Big|_{RM} f_1(T_c) \tag{4.40}$$

where $(dm/dt)|_{RM}$ is the riming rate for any of the ice categories and the function f_1 of the surface temperature of the ice particle T_c represents the temperature dependence of the process. The Hallet-Mossop mechanism is thought to peak at -5°C, and be about zero above -3°C and below -8°C. Linear interpolation then give (Cotton et al., 1986):

$$f_1(T_c) = \begin{array}{cc} 0; & T_c > 270.16 \\ [(T_c - 268.16)/2]; & 270.16 \geq T_c \geq 268.16 \\ [(T_c - 268.16)/3]; & 268.16 \geq T_c \geq 265.16 \\ 0; & 265.16 \geq T_c \end{array} \tag{4.41}$$

- Approximately 1 ice splinter is produced for every 250 drops $\geq$ 24 μm accreted onto each graupel particle at -5°C (Mossop, 1976). The ice crystal production rate per particle, based on the continuous growth equation, is then given by (Cotton et al., 1986):

$$P_p(II) = \frac{1}{250}\frac{\pi D_g^2}{4}\overline{v}_g E(g/c_{24}) N_{24} f_1(T_c)$$

where N_{24} is the concentration of cloud droplets greater than 24 μm in diameter, $E(g/c_{24})$ is the collection efficiency for graupel collecting cloud droplets with diameter greater than 24 μm, $\overline{v}_g$ is the mean terminal velocity of the graupel distribution, and D_g is the diameter of the graupel particle.

To derive an estimate of the number of cloud droplets greater than 24 μm, assume a gamma distribution (2.30). Following the derivation in Cotton et al. (1986) , and assuming that the mixing ratio is the model variable, the mass of a mean cloud droplet (m_c) can be calculated. In their derivation they fixed the shape parameter ν, which left the characteristic diameter D_N as the only free parameter of the distribution. The characteristic diameter can be calculated using the formulation for the water content l of the modified gamma distribution given in Table 2 where, for this application, $c = 1$. Note that equation (76) in Cotton et al. (1986) was derived for a distribution specified in radius, and that the power is incorrectly specified as 1/2, which should be 1/3. Now that the distribution is completely specified, the number of droplets greater than any diameter can be determined. It can be written in the following form

$$N_{24} = N_c f_2(D_n)$$

where f_2 is the fraction of area under the distribution greater than the cut-off diameter, which is defined by

$$f_2(x) = \frac{1}{\Gamma(\nu)}\int_x^\infty X^{\nu-1}\exp(-X)dX = 1 - \Gamma(\nu, x)/\Gamma(\nu),$$

where $x = (D_{24}/D_n)$, $X = (D/D_n)$ and D_n is defined as

$$D_n = \left[\frac{6m_c\Gamma(\nu)}{\pi\Gamma(\nu+3)}\right]^{1/3} \tag{4.45}$$

using the normalized version given for the liquid water content in Table 2.

It can be questioned whether both these processes are independent processes or just different steps in interpretation of the Hallet-Mossop experiments. If this is the case, then $P_p(I)$ and $P_p(II)$ could to some degree be double counting the same process. Cotton et al. (1986) , argued that in that case it would be desirable to use $P_p(II)$ as the only multiplication process.

4.6 Vapor deposition

The governing equation for vapor depositional growth is routinely derived in standard cloud physics textbooks (see Byers, 1965, Pruppacher and Klett, 1978 or Ludlam, 1980 for example), and it can be written in the following form

$$\frac{dm}{dt} = 4\pi CG(T,p)(S-1)$$

where

$$\frac{1}{G(T,p)} = \frac{L^2}{KR_vT^2} + \frac{R_vT}{D_ve_{sat}}$$

In these formulations D_v is the vapor diffusivity coefficient and K is the thermal diffusivity coefficient in air. The shape factor C is D/π for hexagonal plates, or $D/2$ for spherical particles. S is the degree of supersaturation relative to the phase of the particle, T is the environmental temperature, e_{sat} is the saturation vapor pressure, L is the latent heat associated with the process and R_v is the moist gas constant.

When a particle becomes large enough to have a free-fall speed of a few centimeters per second or more, the vapor density gradient is increased ahead of the particle, and the rates of heat and mass transferred are also increased. The effect of ventilation on the mass transfer of vapor from a particle in air can be expressed in terms of ventilation coefficient f_v defined by

$$\frac{dm}{dt} = f_v\left(\frac{dm}{dt}\right)_0$$

where dm/dt is the evaporation rate of a moving particle and subscript 0 indicates evaporation rate of a stationary particle.

Based on the results reported in the literature (Pruppacher and Klett, 1978) the ventilation coefficient for spherical water drops may be written as

$$f_v = \alpha + \beta(\frac{\nu_a}{D_v})^n Re^m \tag{4.49}$$

where α, β, n, m are coefficients and Re is the Reynolds number. The ratio ν_a/D_v is defined as the Schmidt number Sc. Beard and Pruppacher (1971) , give the following expressions

$$f_v = 1.00 + 0.108\left(\mathrm{Sc}^{1/3}\mathrm{Re}^{1/2}\right)^2$$

for $\mathrm{Sc}^{1/3}\mathrm{Re}^{1/2} < 1.4$, and

$$f_v = 0.78 + 0.308\mathrm{Sc}^{1/3}\mathrm{Re}^{1/2}$$

for $\mathrm{Sc}^{1/3}\mathrm{Re}^{1/2} > 1.4$ Assuming $\mathrm{Sc} = 0.71$ (as did Beard and Pruppacher, 1971) we get

$$f_v = \begin{cases} 1.00 + 0.086\mathrm{Re} & for \ \ \mathrm{Re} < 2.5 \\ 0.78 + 0.275\mathrm{Re}^{1/2} & for \ \ \mathrm{Re} > 2.5 \end{cases}$$

The ventilation coefficients of ice are poorly known. For several years we were using the formula given by

$$f_v = 1.0 + 0.297\mathrm{Re}^{1/2}.$$

Cotton et al. (1982) defined the ventilation coefficient as

$$f_v = 1.0 + 0.229\mathrm{Re}^{1/2}. \tag{4.54}$$

This formulation of the ventilation coefficient is used for both the water and ice phase, and is still used in CSU-RAMS.

A distribution mean value for the ventilation coefficient may be obtained by multiplying (4.49) by the distribution function and integrating over the size spectrum. If we assume that the Schmidt number Sc is a constant, as in (4.52), (4.53) or (4.54), the Reynolds number as given in (4.11) and the terminal velocity of the form of (4.10), we get the general formulation of

$$\overline{f_v} = \alpha + \beta S_c[Re(D_n)]^m F(m[p_v + 1]) \tag{4.55}$$

If a basic assumption in a model is that the supersaturation with respect to water will remain zero, then it has to be assumed that the excess vapor, not consumed by vapor deposition on all the other categories, have to go to the cloud water category. The total amount of excess water, assuming moist adiabatic ascent, was given by Tripoli and Cotton (1980) :

$$\frac{dm}{dt}\Big|_c = \frac{wg\overline{r}_{sat}}{RT_v}\left(\frac{\varepsilon L_s}{c_p T} - 1\right) \Big/ \left(\frac{\varepsilon L_s^2 \overline{r}_{sat}}{Rc_p T^2} + 1\right) \tag{4.56}$$

This equation will give the total amount of excess vapor, the vapor consumed by the other categories will then be subtracted from this amount.

4.7 Surface temperature of hydrometeors

Under the assumption that each hydrometeor is in thermal equilibrium such that the rate of heat released by vapor deposition and freezing is balanced by the rate of diffusion of heat from the particle surface, an evaluation of the surface temperature of the particle surface can be made.
leads to an expression of the surface temperature as a function of the rate of vapor deposition and riming

$$T_{sfc,i} - T = \frac{1}{4\pi C K f_v}\left(L_s \frac{dm}{dt}\Big|_{VD} + L_f \frac{dm}{dt}\Big|_{CL}\right) \tag{4.57}$$

where the subscript VD refers to vapor deposition and CL refers to collection.

4.8 Coagulation: collision and coalescence

In this section we will look at the collection growth processes, where water categories grow by the collection of other water categories. The different water categories may be distributed according to different probability density functions.
The average number of particles with diameters between $D_x + dD_x$ collected per unit time by a single droplet D_y is given by

$$\pi\left(\frac{D_x}{2} + \frac{D_y}{2}\right) \quad v_x(D_x) - v_y(D_y) \quad n_x(D_x)E(x,y)dD_x$$

where E(x,y) is collision efficiency of water class x colliding with water class y. The mass increase of the particle D_y is then given by (4.58) multiplied by the mass $m_x(D_x)$. Integrating over all particles in class x gives the average mass change of single particle of diameter D_y.

$$\int_0^\infty m_x(D_x)\pi\left(\frac{D_x}{2}+\frac{D_y}{2}\right)^2 \mid v_x(D_x)-v_y(D_y)\mid n_x(D_x)E(x,y)dD_x \tag{4.59}$$

Finally, taking into account that class y is a collection of different sized particles, we get the mixing ratio change of class y due to collection with class x

$$CL_{xy}=\frac{1}{\rho_0}\frac{\pi}{4}\int_0^\infty\int_0^\infty m_x(D_x)(D_x+D_y)^2 \quad v_x(D_x)-v_y(D_y) \quad n_x(D_x)n_y(D_y)E(x,y)dD_xdD_y. \tag{4.60}$$

where CL_{xy} refers to the collection of category x by category y. The absolute value of difference in terminal velocities in (4.60) makes the integration cumbersome and several approximations have been proposed in the past. In this section four different methods of evaluating (4.60) will be discussed. In all the methods it is assumed that an average value for the collection efficiency exits and is known.

4.8.1 The continuous growth equation

In this section we consider the collection process whereby small cloud particles are collected by other particles. The assumptions made are that the terminal velocity of the small cloud particles (x) is small in comparison with the typical terminal velocity of class of larger particles (y), as well as that the diameter of the smaller particle may be neglected in comparison with that of the larger particle. The change in mass of a single particle is then given by

$$\left.\frac{dm}{dt}\right|_y=\frac{\pi}{4}D_y^2v_y(D_y)\overline{E}(x,y)\rho_0\overline{r}_x \tag{4.61}$$

where $\overline{r}_x$ is a cloud particle mixing ratio. Using this solution we can write a approximation for (4.60) as

$$CL_{xy}=\frac{1}{\rho_0}\frac{\pi}{4}D_{ny}^2v_y(D_{ny})\overline{E}(x,y)\rho_0\overline{r}_xN_{ty}F(p_{vy}+2) \tag{4.62}$$

This approximation will only be valid for large particles collecting small particles. All the following approximations are valid for similar sized particles collecting each other.

4.8.2 Mean droplet terminal velocity

In this approximation we assume that the terminal velocity difference $\mid v_x(D_x) - v_y(D_y) \mid$ can be replaced by the constant value $v_x(D_{nx}) - v_y(D_{ny}) \mid$. We can then write (4.60) as

$$CL_{xy} \approx \frac{1}{\rho_0}\frac{\pi}{4}\overline{\Delta v}_{xy}\overline{E}(x,y)I$$

where

$$I = \int_0^\infty \int_0^\infty m_x(D_x)(D_x + D_y)^2 n_x(D_x) n_y(D_y) dD_x dD_y.$$

and $\overline{\Delta v}_{xy}$ is

$$\overline{\Delta v}_{xy} = \mid v_x(D_{nx}) - v_y(D_{ny}) \mid .$$

The integral I can easily be evaluated analytically following the procedures discussed in previous parts of this document. Assuming a mass-diameter relationship of the form of (4.3) we get after some simple algebra

$$I = N_{tx} N_{ty} m_x(D_{nx}) C_{xy}$$

where the constant C_{xy} is given by

$$C_{xy} = D_{nx}^2 F_x(p_m + 2) F_y(0) + 2 D_{nx} D_{ny} F_x(p_m + 1) F_y(1) + D_{ny}^2 F_x(p_m) F_y(2).$$

The functions F_x and F_y depend on the distribution and are summarized in Table 2. Combining (4.63) and (4.66) we get

$$CL_{xy} \approx \frac{1}{\rho_0}\frac{\pi}{4}\overline{\Delta v}_{xy}\overline{E}(x,y) N_{tx} N_{ty} m_x(D_{nx}) C_{xy} \tag{4.68}$$

Weighted root mean square (RMS) terminal velocity

Again we assume that the velocity difference can be replaced by a constant value $\overline{\Delta v_{xy}}$. The mathematical formulation of the solution will thus remain the same as (4.63). But this time we define the velocity difference in the following manner

$$\overline{\Delta v_{xy}^2} = \frac{I_v}{I} \tag{4.69}$$

where I_v is defined by

$$I_v = \int_0^\infty \int_0^\infty [v_x(D_x) - v_y(D_y)]^2 w_{xy} dD_x dD_y \tag{4.70}$$

$$I = \int_0^\infty \int_0^\infty w_{xy} dD_x dD_y \tag{4.71}$$

Notice that the integral I in the numerator of (4.69) is given by (4.64). Thus, the weighting function is defined by

$$w_{xy} = m_x(D_x)(D_x + D_y)^2 n_x(D_x) n_y(D_y). \tag{4.72}$$

After some algebra we obtain as a solution for I_v the following expression

$$I_v = N_{tx} N_{ty} m_x(D_{nx}) \left[v_x^2(D_{nx}) C_1 - 2 v_x(D_{nx}) v_y(D_{ny}) C_2 + v_y^2(D_{ny}) C_3 \right] \tag{4.73}$$

where C_1, C_2 and C_3 are coefficients which can be written in vector notation as

$$\mathbf{C} = \mathbf{F}\mathbf{D}. \tag{4.74}$$

The 3×3 matrix $\mathbf{F}$ of coefficients is given by

$$\begin{bmatrix} F_x(2p_{vx} + p_{mx} + 2) F_y(0) & F_x(2p_{vx} + p_{mx} + 1) F_y(1) & F_x(2p_{vx} + p_{mx}) F_y(2) \\ F_x(p_{vx} + p_{mx} + 2) F_y(p_{vy}) & F_x(p_{vx} + p_{mx} + 1) F_y(p_{vy} + 1) & F_x(p_{vx} + p_{mx}) F_y(p_{vy} + 2) \\ F_x(p_{mx} + 2) F_y(2p_{vy}) & F_x(p_{mx} + 1) F_y(2p_{vy} + 1) & F_x(p_{mx}) F_y(2p_{vy} + 2) \end{bmatrix} \tag{4.75}$$

and the 3×1 column vector $\mathbf{D}$ is defined by

$$\mathbf{D} = (D_{nx}^2, 2D_{nx}D_{nx}, D_{nx}^2)^T \tag{4.76}$$

Finally, if we define another 1×3 row vector $\mathbf{V}$

$$\mathbf{V} = \left[v_x^2(D_{nx}), -2v_x(D_{nx})v_y(D_{ny}), v_y^2(D_{nx})\right], \tag{4.77}$$

then we can write CL_{xy} in a concise way as

$$CL_{xy} \approx \frac{1}{\rho_0}\frac{\pi}{4}\overline{E}(x,y)N_{tx}N_{ty}m_x(D_{nx})(\mathbf{V}\cdot\mathbf{FD})^{1/2}. \tag{4.78}$$

4.8.4 The analytical solution

In this section we find the analytical solution to (4.60). Assuming that the terminal velocity can be represented in the form of (4.10) for both the categories, we notice that $v_x(D_x) - v_y(D_y)$ | changes sign when

$$c_{vx}D_x^{p_{vx}} = c_{vy}D_y^{p_{vy}} \tag{4.79}$$

and by simple manipulation of (4.79) we get

$$D_y(x) = f_{xy}D_x^{p_{xy}} \tag{4.80}$$

where

$$f_{xy} = \frac{c_{vx}}{c_{vy}},\ p_{xy} = \frac{p_{vx}}{p_{vy}} \tag{4.81}$$

By doing partwise integration with respect to y such that the velocity difference has the same sign over each part, we can write

$$CL_{xy} \approx \frac{1}{\rho_0}\frac{\pi}{4}\overline{E}(x,y)J \tag{4.82}$$

where

$$J = \int_0^\infty m_x(D_x)(J_1 - J_2)n_x(D_x)dD_x \tag{4.83}$$

The integrals J_1 and J_2 are given by

$$J_1 = \int_0^{D_y(x)} (D_x + D_y)^2 \left[v_x(D_x) - v_y(D_y)\right] n_y(D_y) dD_y \tag{4.84}$$

$$J_2 = \int_{D_y(x)}^{\infty} (D_x + D_y)^2 \left[v_x(D_x) - v_y(D_y)\right] n_y(D_y) dD_y \tag{4.85}$$

Integrating (4.84) we get

$$\begin{aligned} J_1 \;=\; & \Big\{ v_x(D_x) \left[D_x^2 G_1(0, D_y(x)) + 2 D_x D_{ny} G_1(1, D_y(x)) + D_{ny}^2 G_1(2, D_y(x)) \right] - v_y(D_{ny}) \\ & \times \left[D_x^2 G_1(p_{vy}, D_y(x)) + 2 D_x D_{ny} G_1(p_{vy}+1, D_y(x)) + D_{ny}^2 G_1(p_{vy}+2, D_y(x)) \right] \\ & \Big\} \times N_{ty}. \end{aligned} \tag{4.86}$$

In this equation the form of the function G_1 is summarized in Table 3. The integral (4.85) has the same form as (4.86) but with G_1 replaced by G_2. The functions $G1$ and $G2$ are expressed in terms of the incomplete gamma functions, and are dependent on D_x. The integral (4.83) is thus not trivial to solve, but it can be done, at least numerically, as is shown in appendix D.

4.8.5 Coalescence efficiency

Another important parameter to be considered in the coagulation growth equation, is the collection efficiency E. The collection efficiency contains two principle components; one the hydrodynamic efficiency or the probability of collision and secondly the coalescence efficiency or the probability that two colliding particles will stick.

It is common in bulk microphysical models to set the collection efficiency for cloud droplets or raindrops, to any other category, to 1. It is also generally assumed that the collision efficiency is 1 for all categories. The coalescence efficiency for ice-ice interactions are difficult to treat theoretically, and generally are parameterized from observational or laboratory studies. The results of these studies are somewhat confusing since the experiments reported by Hallgren and Hosler (1960) , and Hosler and Hallgren (1960) showed a clear temperature dependence. On the other hand, Latham and Saunders (1971) , found no such temperature dependence in their laboratory experiments. It has been suggested by Cotton et al. (1986) that the delicately branched dendrites yields the

highest coalescence efficiencies. Passarelli and Srivastav (1979) inferred from aircraft observations a coalescence efficiency of 140% for large ice crystals or aggregates in the temperature range $-12°C$ to $-15°C$.

Cotton et al. (1986) , approximate Hallgren and Hosler's results with a temperature dependent coalescence efficiency formula:

$$\mathrm{EF}(T) = \min\left[10^{0.035(T-273.16)-0.7}, 0.2\right], \tag{4.87}$$

where T represents the surface temperature of the ice crystal, graupel or aggregate. In this formulation the maximum value for the coalescence efficiency will be 20%. For aggregates collecting crystals, they assumed that the aggregate temperature determines the efficiency, while for graupel collecting aggregates they assumed that the warmer of the two determines the efficiency. However, in the temperature range $-12°C$ to $-15°C$ the collection efficiency is set to 140% to conform to Passarelli and Srivastava (1979) .

Melting of ice particles

The heat balance at the surface of an ice particle falling through a cloudy atmosphere growing through vapor deposition and riming of cloud water (and rain water – only for aggregates and graupel), is given by Cotton et al. (1986) :

$$L_f \frac{dm}{dt}\Big|_{melt} = -2\pi D f(Re)[K(T-T_f)+L_s D_v(\rho_v-\rho_{vs}(T_f))] - \left[\frac{dm}{dt}\Big|_{RM} + \frac{dm}{dt}\Big|_{CL}\right] c_w(T-T_f) \tag{4.88}$$

where T_f is the freezing temperature 273.16 K. For snow the $(dm/dt)_{CL}$ term should be neglected, since snow will not collect rain.

Now, in a large model, the vapor depositional growth may be calculated before melting is considered. This knowledge may be used in the following manner (Tripoli, personal communication). If the estimate of the latent heat released due to vapor deposition is taken from the previous calculated rate which was calculated at the environment temperature, then an additional term should be included in the sensible heat transfer term to bring the vapor deposition estimate to T_f. The resultant heat balance equation will then be

$$L_f \frac{dm}{dt}\Big|_{melt} + L_s \frac{dm}{dt}\Big|_{VD} = -2\pi DKf(Re)(T - T_f) - \left[\frac{dm}{dt}\Big|_{RM} + \frac{dm}{dt}\Big|_{CL} + L_s \frac{dm}{dt}\Big|_{VD}\right] c_w(T - T_f)$$

where again for categories that do not collect rain the $(\frac{dm}{dt})_{CL}$ term needs to be neglected.

4.10 Auto-conversion

One more process needs to be considered, and that is the process through which cloud particles grow, through self-collection or diffusional growth, into a precipitation category.

4.10.1 Cloud droplets to raindrops

It used to be considered that the most important ingredient for self-broadening of the cloud droplet spectrum is the initial droplet spectrum as well as the liquid water content and time available for collection. Recent studies have suggested that turbulent inhomogeneous mixing, or ultra giant aerosols are important to self-broadening. These theories are however themselves still in a turbulent stage, with the basic processes not well understood. Therefore most parameterizations are still based on the work of Berry and Reinhardt (1974a,b,c,d) ,b,c,d, or Kessler (1969) .

Manton and Cotton (1977) , suggested a scheme for the auto-conversion of cloud droplets to rain based on a threshold average diameter in the droplet distribution. They suggested that this parameterization was an improvement on the Kessler (1969) , parameterization of the same process. This was expressed in the form

$$\frac{dm}{dt}\Big|_r = f_c \overline{r}_c h(\overline{r}_c - r_m)$$

where f_c represents the mean collision frequency for cloud droplets which become raindrops after colliding, $h(x)$ is the Heaviside unit step-function and r_m is the minimum cloud water mixing ratio below which there is no conversion. There is a minimum diameter corresponding to this minimum cloud water mixing ratio. They estimated the mean collision frequency as

$$f_c = \frac{\pi}{2} D_c^2 E_c v_c N_c \tag{4.91}$$

where D_c is the mean cloud droplet diameter, E_c is the collection efficiency for this process, and v_c is the terminal velocity of the cloud droplets, given by Stokes Law (4.18). The collision efficiency for droplets as discussed by Scott and Chen (1970) , yields an average value of $E_c = 0.55$.
An alternative procedure to simulate the complete warm rain process was discussed by Clark and Hall (1983) , but this work was never completed. Ziegler (1985) , developed yet another parameterization, including auto-conversion of cloud to rain, accretion of cloud by rain, and large hydrometeor self-collection and break-up. His parameterization was based on gamma distributed cloud and rain populations, and he predicted the mixing ratio and concentration tendencies independently from each other.

4.10.2 Ice crystals to aggregates

The process is even less well understood. A parameterization suggested by Cotton et al. (1986) will be discussed. A simple model for the conversion rate was derived by considering the rate of collection amongst a homogeneous population of ice crystals which is given by

$$\frac{dN_i}{dt}\Big|_{agg} = -K_i N_i^2$$

where N_i represents the concentration of pristine crystals and K_i is the collection kernel. conversion rate of ice crystal mixing ratio to aggregates due to self-collection is then given by

$$\frac{dr_i}{dt}\Big|_{agg} = K_i N_i r_i$$

To obtain an estimate for K_i they adapted the Passarelli and Srivastava (1979) , stochastic collection kernel model which estimates K_i based on a distribution of particle densities for equal-sized crystals. This gives

$$K_i = \frac{\pi}{6} D_i^2 v_i E_i X \tag{4.94}$$

where X is proportional to the variance in particle fall speed. Passarelli and Srivastava (1979) , gave a best estimate of $X = 0.25$. Cotton et al. (1986) , suggest that this be adjusted for different cases to calibrate K_i for specific cases.

This parameterization differs from the Lin et al. (1983) , parameterization in that theirs is based on the Kessler (1969) , warm rain parameterization. In that case the conversion rate is a linear function of the mixing ratio of ice crystals and a rate parameter which varied with temperature to simulate variations in collection efficiency such as discussed in the above section on collection efficiency. In the Cotton et al. (1986) , aggregation parameterization, the conversion rate also varies linearly with the mixing ratio of the ice crystals, but it also depend on N_i and K_i. As a result the conversion rate exhibits a strongly non-linear dependence on the characteristics of the ice crystal population, and particularly the concentration of ice crystals.

Part III
DOCUMENTATION OF THE RAMS MICROPHYSICAL PARAMETERIZATION SCHEME

5 Introduction

The Colorado State University Regional Atmospheric cloud Modeling System bulk microphysical parameterization will be discussed based on the equations and ideas developed in the previous sections. The concepts and parameterization were developed in a very general sense, now the specific schemes will be presented as they have been implemented in the model code. The model is still in the process of development so that the purpose of this description is to provide a basis from which the continued work may proceed. This description is valid for the code as its was in early 1989.

The basic philosophy behind the development of the code was to have the flexibility to change formulation of the parameterization scheme of the model for different applications. Historically the number of categories of hydrometeors and the size-distribution of the hydrometeors assumed in a model vary from investigator to investigator. It seems that there is an almost infinite set of combinations of particle size distributions, particle size distribution parameters, and hydrometeor types that can be formulated in a cloud model. With the mathematical considerations presented in Part 1 of this document, a generalized bulk microphysics parameterization capable of meeting this challenge of greater flexibility can be developed.

The current version of the model has as its primary prognostic microphysical variables the mixing ratios of rain, pristine ice, snow, aggregates and graupel/hail. The number concentration of pristine ice crystals is also predicted while the prediction of the concentrations for the other species is only partially implemented. The mixing ratio of water vapor and cloud droplets is diagnosed. At this stage the generalized distribution function approach has not been fully implemented yet. In general, the cloud droplet size distribution is not specified although it is assumed it is distributed in a gamma distribution in order to predict secondary ice crystal production. Ice crystals are assumed to be monodispersed, while all the other categories are distributed according to the inverse exponential

distribution function. There is some flexibility in the scheme, with cloud droplets the only required hydrometeor class, whereas the rest are all optional. The investigator has the further option of deciding on how the various parameters of the distributions are to be treated by the model. Either the slope or the intercept of the inverse exponential distribution function may be held constant, while the other is predicted, or both may be predicted independently. The parameter held constant by the investigator needs to be specified. No hydrometeor class is dependent on any other class for its existence, nor on the assumed distribution of any other class, or the selected option of the distribution parameter. This leaves the investigator with a large degree of flexibility in selecting a microphysics parameterization that is optimized for the specific application in mind, such as a regional-scale numerical study versus a small continental cumulus simulation.

Even though the mixing ratios of water vapor and cloud droplets are diagnosed by the model, they are treated in the microphysics package together with the other categories. This was necessary to compute the interaction of these two categories with all the others. How the mixing ratios for these two categories are derived, will be discussed in the next part of the paper.

The software engineering aspects of the model will be ignored in this discussion, instead only consideration of the physics will be given. The general flow of the model will be retained, with reference to the specific subroutines where the various physical processes are treated.

All processes in the model, and all constants, are given in cgs-units, thus all lengths are in centimeters, all weights are in grams and time is given in seconds. All derived units are also in these basic units.

6 Bulk microphysical parameterization

6.1 The namelist input

In the current formulation of the model, the user has several options that may be set in the input namelist. These options include what water categories are activated, as well as specifying what variables are predicted (ie mixing ratio and/or concentration). The user further has to specify the number of cloud droplets per unit volume that is to be used in simulation (CON) and the minimum crystal mass (AMIO). Currently all the distributions for the various categories are fixed, in RAMS as either constant or exponential distributions. The cloud droplet category is always activated whenever the microphysics are activated, as is the vapor category. The user has the option whether

to activate the rain, pristine ice crystals, snow, aggregates and graupel categories. The model will function with any number of the categories activated, whether or not it is physically realistic has to be decided by the user. The current assumed distributions are: unspecified for cloud droplets, monodisperse for the pristine ice distribution, and exponential for the rain, snow, aggregate and graupel distributions. The user may also specify what parameters of the distribution are to be predicted, diagnosed or held constant. With the exponential distribution there are two degrees of freedom and the current formulation allows several ways this may be determined. The user may choose between:

1. Mixing ratio predicted, while the distribution parameters are diagnosed from default mean diameters. These values are given in table 6.

2. Mixing ratio predicted, and the investigator has to specify the mean diameter of the distribution. The total concentration will then be diagnosed.

3. Mixing ratio predicted, and the investigator has to specify the intercept. The mean diameter and total concentration of the distribution will then be diagnosed.

4. Mixing ratio predicted, and the investigator has to specify the total concentration. The mean diameter will then be diagnosed.

5. Mixing ratio and concentration predicted, mean diameter diagnosed.

These options are set by the five variables (NIRCNFL), (NIPCNFL), (NISCNFL), (NIACNFL) and (NIGCNFL). Depending on the option specified here, the user has to give a value for the parameter that is held constant (if any). These values have to be specified in cgs units. Once again, it is up to the user to determine whether these values are physically plausible, although the model does have certain bounds on the parameters, it will default without giving warning messages. Some caution about concentration predictions should be given. Only the pristine ice concentration prediction has been tested, the concentration prediction for the other categories has been implemented, but has not yet been thoroughly tested.

6.2 The driver

The driver subroutine (MICPHYS) is the routine called from the dynamical model. The code was developed in such a way that the microphysics package may be called from any dynamics package. This requires that all the model variables need to be passed to the microphysics package, which will then calculate the microphysical tendencies due to interaction between the various hydrometeor categories, i.e. the source/sink terms in the continuity equations for the water substance included in the model. The total concentration and mixing ratio tendencies for all the categories of hydrometeors are then passed back to the dynamical model.

The model variables needed by the microphysics package are: The water vapor mixing ratio, the ambient dry air density, pressure, temperature, local vertical temperature gradient and the vertical motion of the air at each grid point where microphysical calculations are to be performed. The microphysical variables required from the dynamic model are the total concentration and mixing ratio for all the user specified categories. The user specified options for the prognostic distribution parameters are also passed, as well as the user specified constants. Currently the only user specified constant is the minimum mass that any ice crystal may have. It is envisioned that this will be increased. Finally, some engineering variables are also passed.

The flow through this routine is simple. First, all the physical parameters needed are calculated (SOMTHNGS). Then a call is issued to a routine that builds a standard set of descriptive parameters for each category (DIAGNOSE), which contains information about the distribution type, the habit, the name and the functional dependence of mass, density and terminal velocity on diameter. These first two routines set up required physical variables and customized arrays based on user-specified options for the microphysics for use in the following general routines.

Next, the routine for calculating all the microphysical tendensies is called (MTEND). Since all the calculations are performed independently of each other and are summed afterwards, at times more than what is available in a category may be consumed. These processes are not necessarily independent, and there is no clear indication as to which processes will be preferred over other processes, or how they may non-linearly interact. Based on the above, another routine (MDLTEND) is called which adjusts the tendencies such that all categories will remain positive definite at each grid point. After these corrections have been made, control is passed back to the dynamic model.

6.3 Physical parameters

It this section, the steps followed in routine (SOMTHNGS) will be followed through. This routine is just a driver routine which calls several other routines. Various quantities that are used throughout the microphysics package are calculated in this routine.

First, the Heaviside step function for temperature dependence is calculated (HEAVSTEP). function is used to discriminate between above and below freezing ambient temperatures. function is very simple, it is simply set to 1 if the temperature is less that 0°C, and 0 otherwise. Then the saturation value over water and ice is calculated for all the grid points in the microphysics vector. This is accomplished through calls to the subroutines (QSPCGS), (ICESAT) and (WATSAT). The routine (QSPCGS) calculates the saturation vapor pressure over water and ice, following the procedure outline by Derickson and Cotton (1977) . Once the saturation vapor pressure is known, the saturation mixing ratio (the model variable is mixing ratio) can easily be calculated using the formula

$$r_{sat(,i)} = \frac{\epsilon e_{sat(,i)}}{p - e_{sat(,i)}}$$

where r is the mixing ratio, p the pressure, e the vapor pressure and $\epsilon = 0.622$. When the temperature is above 0°C, the saturation mixing ratio with respect to ice is taken as the value with respect to water.

The dynamic viscosity, thermal conductivity and the vapor diffusivity are next calculated by calls to the routines (XDVISC), (XXK) and (XDFV). The dynamic viscosity is calculated according to

$$\frac{\mu_d}{\mu_0} = \frac{T_0 + C}{T + C}\left(\frac{T}{T_0}\right)^{3/2} \tag{6.2}$$

where T is the temperature in °K, μ_0 is the dynamic viscosity at a temperature T_0, and C is a constant ($C = 120$K). At $T_0 = 273$ °K, $\mu_0 = 1.718$ poise. The thermal conductivity and the vapor diffusivity are calculated by interpolation of the List (1968) , data. These values are valid for a temperature range for -40°C to 40°C. The correction for reduced pressure required for the vapor diffusivity calculation is not added in the (XDFV) routine, but is rather included in the following call to (XGTPD).

The term $G(T,p)$ in the vapor deposition growth equation is calculated next with the call to (XGTPD). This term is defined by (4.47) in part 2 of this document. The pressure correction for

Category	Name	Phase	Distribution	Prediction Option	Habit	Mass Coefficient	Mass Power	Vert. Vel. Power
Cloud	ICLOUD	LIQ	CONSTANT	FIXED	SPHE	$\pi/6$	3.0	2.0
Rain	IRAIN	LIQ	IE	USER	SPHE	$\pi/6$	3.0	0.5
Pristine (small)	IPRIS	ICE	CONSTANT	USER	HEX	3.77×10^{-4}	2.0	1.0
Pristine (medium)	IPRIS	ICE	CONSTANT	USER	HEX	2.7126×10^{-3}	2.0	1.0
Pristine (large)	IPRIS	ICE	CONSTANT	USER	HEX	5.28×10^{-3}	2.4	1.0
Snow	ISNOW	ICE	IE	USER	HEX	5.28×10^{-3}	2.4	0.25
Aggregates	IAGG	ICE	IE	USER	SPHE	$0.015 \times \pi/6$	2.4	0.2
Graupel	IGRAUPEL	ICE	IE	USER	SPHE	$0.9 \times \pi/6$	3.0	0.5

Table 5: The RINFO array as it is currently inplemented in the model. The distribution can only be a constant distribution or an inverse exponential distribution (IE). The predition option indicate whether the investigator has an option of prediction parameter (see text). Allowable habits are only spherical or hexigonal.

the vapor diffusivity is done in this routine. The term is calculated for both the liquid and the ice vapor deposition modes at each grid point.

Finally, a call is made to a routine that sets a look-up table that is used for the integration of the distributions. Currently in RAMS only calculations for the exponential distribution function is tabulated.

6.4 Distribution diagnostics

This is the second call from the driver subroutine. The first call calculated some of the physical values needed for the microphysics calculations, this routine will now translate the model variables into distribution parameters, since the microphysics is prognosed for the distribution parameters. Once again this routine is just a driver routine calling a series of subroutines, one for each water category.

The characteristic diameter and the total concentration for each category is diagnosed from the mixing ratio and the concentration [(DIAN0), (DIANT) and (NTDIA)]. These routines utilize equations (4.24) and (4.25) to diagnose either the diameter from a concentration value [(DIAN0) and (DIANT)] or the total number concentration from a given diameter. For the constant distributions the number concentration will be specified, and the mean diameter diagnosed. Thus, the cloud water category may have a different diameter at each grid.

The various distribution characteristics for the different categories are also set in this routine. The information array for each category is built in this section. This array contain the following

Category	Parameter	Value
Cloud	Concentration	300
Rain	Diameter	0.054
Pristine	Concentration	$\min(10^{-8}, 10^{-8}\exp[0.6T_s])$
Snow	Diameter	0.1
Aggregates	Diameter	0.33
Graupel	Diameter	0.1

Table 6: Default values set in the model with the user prediction option 1.

information: the name of the category, the phase, the distribution type, the parameter prediction flag, the habit of the category, and the constants and power values of the mass and terminal velocity power relationships. Table 5 gives a summary of how the variables currently are set in the model. The prediction option "user" refers to the distribution flag set by the user in the namelist.

The model provides for three size classes in the pristine category: small, medium and large. These size classes differ in mass-diameter relationships, depicted in Table 5. The decision on what mass-diameter relationship will be used in the calculation of the density and mean diameter is made by calculating the mass of a single ice crystal and then use mass criteria of 10^{-7}g and 10^{-5}g as the two division values.

All the ice categories have limitations on the mean diameter of the distribution. When the distribution obtains a mean diameter out of bounds, it is set at the bound and the number concentration is recalculated. These bounds are given in Table 7. The investigator has some control over the lower bound, in that the variable $PMAS$ is a option that needs to be declared in the input namelist. The upper bound was derived by Cotton et al. (1986) , from the Rogers (1973) , data, and it implies that a breakup mechanism is able to maintain a constant slope in the inverse exponential distribution. The user has to carefully consider this if he decides to predict the number concentration of that category as well.

The mass-weighted distribution mean value of the vertical velocity is calculated in a call to (CALVT). The equations used in this routine were developed in Sections 4.1.3 and 4.2 in part II of this document. The various constants in the equations are defined in Table 8. The variables are defined as follows, β_1, β_2 and α_1 are the coefficients of density, terminal velocity and mass respectively, while P_D, P_VT and P_M are the powers of the density, terminal velocity and mass respectively of

Category	Max. density allowed	Min. mean diameter	Max. mean diameter
Pristine	0.1	$(PMAS/\alpha_1)^{\frac{1}{P_M}}$	$0.33cm$
Snow	0.1	$(PMAS/\alpha_1)^{\frac{1}{P_M}}$	$0.33cm$
Aggregates	0.1	$(\rho_{max}/\beta_1)^{\frac{1}{P_D}}$	$0.33cm$
Graupel	0.9	$0.054cm$	$1.0cm$

Table 7: Density and mean diameter bounds employed in the model.

Category	β_1	P_D	β_2	P_{VT}	α_1	P_M	C_D
Cloud	1.0	0.0	$(\beta_1 g)/(18\mu)$	2.0	$\pi/6$	3.0	–
Rain	1.0	0.0	$CNST$	0.5	$\pi/6$	3.0	0.588
Pristine	$6\alpha_1/\pi$	$P_M - 3$	3.04×10^5	1.0	3.77×10^{-4}	2.0	–
Snow	$6\alpha_1/\pi$	$P_M - 3$	1.53×10^5	0.25	5.28×10^{-3}	2.4	–
Aggregates	0.015	$P_M - 3$	$CNST$	0.2	$\beta_1\pi/6$	2.4	1.3
Graupel	0.9	0.0	$CNST$	0.5	$\beta_1\pi/6$	3.0	0.45

Table 8: Summation of the power law relationships used in the calculation of the terminal velocity for the various categories. The variable $CNST$ is defined in the text.

the diameter power law (see Section 4.1). The coefficients for spherical categories are derived in (4.13) and (4.18). The variable $CNST$ is defined by

$$CNST = \left(\frac{4}{3}\frac{\rho g \beta_1}{\rho_a C_D}\right)^{1/2}$$

The constant drag coefficient used for the bigger spherical categories are also included in this table. Based on (4.23) the vertical velocity of a particle of characteristic diameter (mean diameter for the inverse exponential distribution) is calculated first, and then multiplied by the functional form which is dependent only on the power values of mass and terminal velocity.

A distribution value for the ventilation coefficient is also calculated in a call to (VENT). calculation is based on the definition of the ventilation coefficient given by Cotton et al. (1982) as in (4.54), and the formulation of (4.55) is used for the calculation of the distribution mean value.

Finally, a surface temperature value and the surface saturation mixing ratios are calculated in (CALTRX). For water substance the surface temperature is assumed to be the environmental temperature, while for ice substance the calculation for the surface temperature is based on (4.57). The rate of growth due to riming is calculated in a preliminary way in this routine by assuming that the terminal velocity and the diameter of the cloud droplets are negligible compared to the collector, and that the coalescence efficiency is 1. Based on this calculated temperature the surface saturation mixing ratio is then calculated by calls to (WATSAT) or (ICESAT), which were discussed earlier. The temperature is a function of the saturation value, which again is a function of the temperature, thus this needs to be an iterative process. For expediency this iterative process is only executed twice.

This brings us to the conclusion of the diagnosis routine. This information is used to define the "R"-array in the model that is defined for all the categories. This array contains the following information about each category:

1. The mixing ratio (g/g)
2. The total concentration (#/cm^3)
3. The distribution mass-weighted mean velocity (cm/s)
4. The distribution characteristic diameter (cm)

5. The average particle density (g/cm^3)

6. The distribution mean ventilation coefficient

7. The surface temperature of the particle

8. The saturation mixing ratio at the surface of the particle

The information in the arrays "RINFO" and the "R" arrays is all the required information needed for the calculations of the conversion tendencies.

6.5 Conversions between categories

Now the call to (MTEND) will be followed. As the other routines called from (MICPHYS), this routine is just another driver routine that calls a variety of routines based on certain conditions. This routine calculates the tendencies of mixing ratios and concentration for all the categories of condensate interacting with each other and the vapor category. This routine calculates the tendencies due to five conversion processes: collection (CALCLXY), vapor deposition [(CALVDVCL) and (CALVCVX)], melting (CALMLXR) and ice crystal production (CALSDVI), (CALPHVI) and (CALSPVI) based on a call to (SUPSATL), which calculates an accurate value for the local supersaturation. The total tendency for each category is then calculated by a linear summation of all the calculated tendencies in (CALCNVSN). Finally a check of the tendencies is made in (REPAIR) to make sure that all categories will remain positive definite when these tendencies are applied over one time step.

6.5.1 Collection

The collection tendencies are calculated for each category in (CALCLXY). This is accomplished by calculation of rate of collection of each category by all the others, i.e. the collection of A by B, as well as the collection of B by A will be calculated. This will result in a tendency for both the mixing as well as the concentration. The equations were developed in section 4.8, with the general equation for the mixing ratio tendency given by (4.60). The weighted RMS terminal velocity method as described in section 4.8.3 was used to solve for the integral. Currently the code is constructed in such a way that only interactions between either two constant distributions, a constant and an inverse exponential distribution or between two inverse exponential distributions

can be considered. The code does not reflect the general formulation of (4.78), but does accomplish the same in a more laborious way. The various terms of the solution is determined in (CALCLXY), (CALAVXVY) and (EFFAB). The last two routines calculate the RMS terminal velocity difference [(CALAVXVY)] and the average collection efficiency [(EFFAB)].

The matrix **F** is calculated only for the first pass through (CALCLXY) since it is only dependent on the power of the mass-diameter and terminal velocity-diameter relationships, which are set in the model. The average collection efficiency is then calculated. This is done in routine (EFFAB).

Results reported by Slinn and Hales (1971) , is used to make an approximation for the collision efficiency at the smaller end of the spectrum. An efficiency of 0.0 is assumed for particles with diameter less that 0.1 μm, and 1.0 for particles with diameter greater that 2.0 μm, while a linear interpolation between the two extremes are used for the range in between. Slinn and Hales (1971) , reported these values for aerosol scavenging, though it is applied to cloud substance for this application.

The coalescence efficiency is calculated in (CALTRX). Where either category is liquid, or if the surface temperature of any ice substance is greater that freezing, it is 1.0. The remainder of the discussion is applicable only if both the categories are ice. For graupel collecting graupel the coalescence efficiency is given by (4.87), which has a upper limit of 20%, irrespective of the surface temperature. Graupel colliding with other ice categories will have the same efficiency as above, provided that the surface temperature of both categories are below 0°C, otherwise it will be 1.

For the snow or pristine categories collecting either the snow or pristine category, coalescence efficiencies are based part on interpretations of observations, and part on very loose arguments. Passarelli and Srivastava (1979) , inferred from observations coalescence efficiencies of 140% in the temperature range -11.5°C to -15.5°C in water saturated environments where the dendritic habit dominates. Thus, under these conditions, the coalescence efficiency is set to 1.4. In other cloud conditions, the maximum of the (4.87) value and the linear interpolation between a maximum value of 1.4 at the maximum cut-off diameter and 0.0 at the minimum cut-off diameter is assumed. In other words, The value given by (4.87) will be the minimum, but for bigger mean diameters the efficiency may be considerably higher. When aggregates collide with pristine, snow or aggregates, the collection efficiency is set to 0.3.

The weighted RMS velocity difference is then calculated in (CALAVXVY), and then finally the collection tendency is calculated in the calling routine (CALCLXY) according to (4.78).

6.5.2 Vapor deposition

Vapor deposition is calculated for each category. First, the amount of available vapor, based on movement along a moist adiabat, is calculated in (CALVDVCL). This calculation is based on (4.56) in Section 4.6. There is a section added in this subroutine which allows for an option of concentration prediction of cloud droplets which is not an option in the model and is therefore dead code. Then there is a section that will reduce the vapor deposition tendency for cloud water with the amount consumed by other processes. The total amount of vapor available for vapor depositional growth of the non-cloud water categories is the excess water vapor with respect to saturated movement along a moist adiabat, as well as the total amount of liquid water in the cloud water category at the beginning of the time step. It is assumed that the cloud water will evaporate to provide the necessary vapor if required. This is even valid for vapor depositional growth of rain, which is also collected, although it should be a miniscule number. In the evaporation case, ie. subsaturation, rain and ice may evaporate. If the model produces more evaporation than the saturation mixing ratio then cloud water will be created.

Routine (CALVDVX) then calculate the vapor depositional growth/evaporation of all the other categories based on (4.48). A check is performed to ensure that no more than half of the available mixing ratio of each category may be evaporated during one time step, or that any category may consume more than half the available vapor. If the concentration is forecasted independently, then in the case of evaporation, this will probably lead to a reduction of the number concentration. For growing particles, no change in the number concentration may be expected.

Smaller particles in the distribution would tend to completely evaporate first. Therefore it is assumed that the calculated mass tendency is applied solely to the small particles. The percentage of the total mixing ratio consumed in one time step by evaporation in the category is calculated. The number concentration tendency is then calculated based on the same percentage reduction of the number concentration over one time step.

6.5.3 Melting

The next process that is considered is melting. The melting is currently being calculated according to (4.89). The melting routine (CALMLXR) is only executed for the ice categories with mixing ratio greater than zero and a surface temperature exactly equal to 273.16 K. This calculation is performed in the model by using the previously calculated collection, vapor deposition and ventilation coefficient. If the melting tendency calculated is negative, then freezing will take place. If the total water substance collected is more than the amount that can be frozen in a time step, then the excess which cannot be frozen, will be shed as rainwater. If the melting tendency calculated is positive, then melting takes place at this rate. It is possible in the model for melting to take place at sub-zero ambient temperatures. This is not realistic, however, and if it occurs probably reflects errors in the calculated thermodynamic budget of the ice particle.

The prediction of the number tendency is made following the same argument that was used for the evaporating case. It is assumed that the calculated mass tendency comes from the smaller particles, and that the larger particles remain unaffected. The percentage of the total mixing ratio consumed in one time step by melting in the category is calculated. The number concentration tendency is then calculated based on the same percentage reduction of the number concentration over one time step.

6.5.4 Nucleation

The nucleation of cloud water is not explicitly considered in the model, but rather, the user is allowed the option to prescribe the number concentration of cloud droplets. If not specified, then the number will default according to Table 6.

Ice nucleation however is explicitly calculated based on the discussion for ice nucleation in Section 4.5 in Part II. Three processes for ice nucleation are considered: sorption/deposition nucleation, phoretic contact nucleation and splintering production (secondary ice production). These processes will only be considered in the model if either of or both the pristine ice or snow categories in the model is activated.

At this point accurate computations of the vapor depositional growth rates of the cloud water have been made. This is used to re-compute the local supersaturation and the cloud droplet temperature

(SUPSATL). If the air is saturated and cloud water exists, then the diffusional growth equation (4.46) is solved for $(S-1)$, while, if the air is sub-saturated, the sub-saturation is calculated from

$$SS = 1 - r/r_{sat}. \tag{6.4}$$

The surface temperature is then recalculated based on (4.57) where for the cloud category $(dm/dt)_{Cl}$ is zero. Finally, based on this temperature, the final saturation mixing ratio over the droplet is calculated.

In all the routines it is assumed that the nucleated ice will grow rapidly in the course of one time step to the user specified minimum ice crystal mass. The sorption/deposition nucleation is considered in (CALSDVI). **If the number concentration is explicitly predicted** (in other words, you must have either the pristine ice activated with option 5, or else the snow activated with option 5 with the pristine ice not in the model), then a expected initial number concentration diagnosed from the Fletcher curve given by (4.28) is calculated. An upper bound of the concentration of 1 (cm^{-3}) is enforced on this value. The Fletcher curve value is then adjusted according to (4.29). In the current version the constant B has been reduced from 3.15 m^{-3} as used in Cotton et al. (1986) , to 1 m^-3. The constants $b = 4.5$ and $a = 0.6$ remain the same. Another limit is placed on the number that can be nucleated, namely that this process may not consume more that 50% of the available water vapor. Now that the number tendency is known, the mixing ratio tendency follows from the assumption that all the crystals grow to the minimum crystal mass in one time step. For the more common case **where only the mixing ratio tendency is forecast**, the mixing ratio tendency is calculated from

$$\left.\frac{dm}{dt}\right|_{sorp} = N_0 w \left.\frac{dT}{dz}\right|_{env} \exp(aT_s) \times \frac{m_{min}}{\rho_a} \tag{6.5}$$

where w is the local vertical velocity, (dT/dz) is the local environment temperature gradient and m_{min} is the minimum ice crystal mass as specified by the user in the input namelist.

Phoretic contact nucleation is considered in (CALPHVI). This process can only operate when there is a coexistence of supercooled cloud water ($T_c < 270.16$ K) and ice, which, in the model, is rare. This routine is derived from Young (1974a) and applied by Cotton et al. (1986) . The equations are reproduced in this document in (4.31 to 4.38). The routine opens with a call to

(AERSTUFF), which calculates the Knudsen number according to (4.37), the number of active contact nuclei according to (4.38) and the aerosol diffusivity according to (4.39). In these equations $N_{a0} = 2 \times 10^{-1}$ and $R_a = 3 \times 10^{-5}$. The aerosol thermal conductivity is also assigned in this routine, it is given the constant value of 5.39×10^4. The contact nucleation is then calculated in (CALPHVI) based on (4.31) to (4.36). The sum of the Brownian, the thermophoretic and the diffusiophoretic diffusion tendencies are then calculated. This is restricted to be a positive definite number, and similar to the sorption tendency, it is not allowed to consume more than 50% of the available vapor over the time step. Again, these crystals are assumed to grow to the minimum crystal size within one time step.

Finally, secondary ice production will be considered. This is calculated in (CALSPVI), a routine which will be called for all the ice categories with the exclusion of the pristine ice category. The calculations are based on (4.40 to 4.45), in other words, both processes are included. For a more detailed explanation and derivation of the equations, see Cotton et al. (1986) , equations (71) through (82). Note that currently the approximation for the function n_2 (f_3 in Cotton et al., 1986) is no longer used, but the integral is analytically evaluated. The dispersion γ_r in the code is now set at 1 instead of 0.18 as in the paper, which makes the assumed cloud droplet distribution an exponential distribution. Similar to the previous nucleation processes, the crystals are assumed to grow by vapor deposition to the minimum crystal mass within one time step. The same restriction that this process may not consume more that 50% of the available vapor also applies here.

6.5.5 Conversions actually applied

At this stage in the model, most of the basic interactions have been calculated, and we are almost in the position to determine the final conversions amongst the categories. This is accomplished through a double loop over all the microphysical categories, calculating sources and sinks for each category through repeated calls to (CALCNVSN).

The basic idea in this routine is to go to each category and look at it as a source. Then a loop is run through all the other categories where they are treated as potential sinks, calculating the net conversion to each. Since the complete arrays of nucleation, deposition, melting and collection tendencies have already been calculated, this can be done. The only basic process still needed is the

auto-conversion routines. These processes are computed in routines (CALCNCR) and (CALCNIA). These routines are actually called from within the major double loop in (CALCNVSN), but it will be discussed here not to break the flow of the discussion of conversion processes later.

The conversion of cloud to rain is the Manton and Cototn (1977) , parameterization discussed in section 4.10.1. The collection efficiency is defined as $E_c = 0.55$ while the minimum diameter corresponding to the minimum mixing ratio is defined as $D_{cm} = 0.002$ cm. This routine is only executed if the cloud mixing ratio is greater that zero, and the cloud droplet diameter at that grid is greater than D_{cm}.

The ice-autoconversion routine is called for the conversion of pristine ice to aggregates and for the conversion of snow to aggregates. The model parameterization is that discussed in section 4.10.2. The collection efficiency for autoconversion is calculated in a call to (EFFAB). The factor X in (4.94) is set to 0.25 in the code.

In order that corrections to the tendencies for excessive transfers can be made at a later stage, it is required that the transfers be positive definite from a source to a sink. All the interactions described in the following sections are summerised in Figure 6.5.5. The effect in the different categories are indicated in the boxes as (r) for changing the mixing ratio and (N) for changing the number concentration. Processes dependent on the inclusion/exclusion of another category are in brackets, with the category on which the process is dependent as a superscript outside the bracket.

1. Vapor as a source

   - To cloud: This occurs by condensation onto cloud droplets. This is done diagnostically based on movement along a moist adiabat.
   - To rain: Although condensation on raindrops can be expected to be small, it is routinely calculated, since the effect of evaporation can be quite important to the simulation. This process will affect only the mixing ratio and not the concentration tendency of the rain drops.
   - To pristine ice: Sublimation of vapor into the pristine ice category occurs both by nucleation and diffusional growth. Since the early growth of pristine ice crystals are fast, it is assumed that all the nucleated crystals grow within one time step to a minimum mass, which is specified by the user. All three the modeled nucleation processes are included.

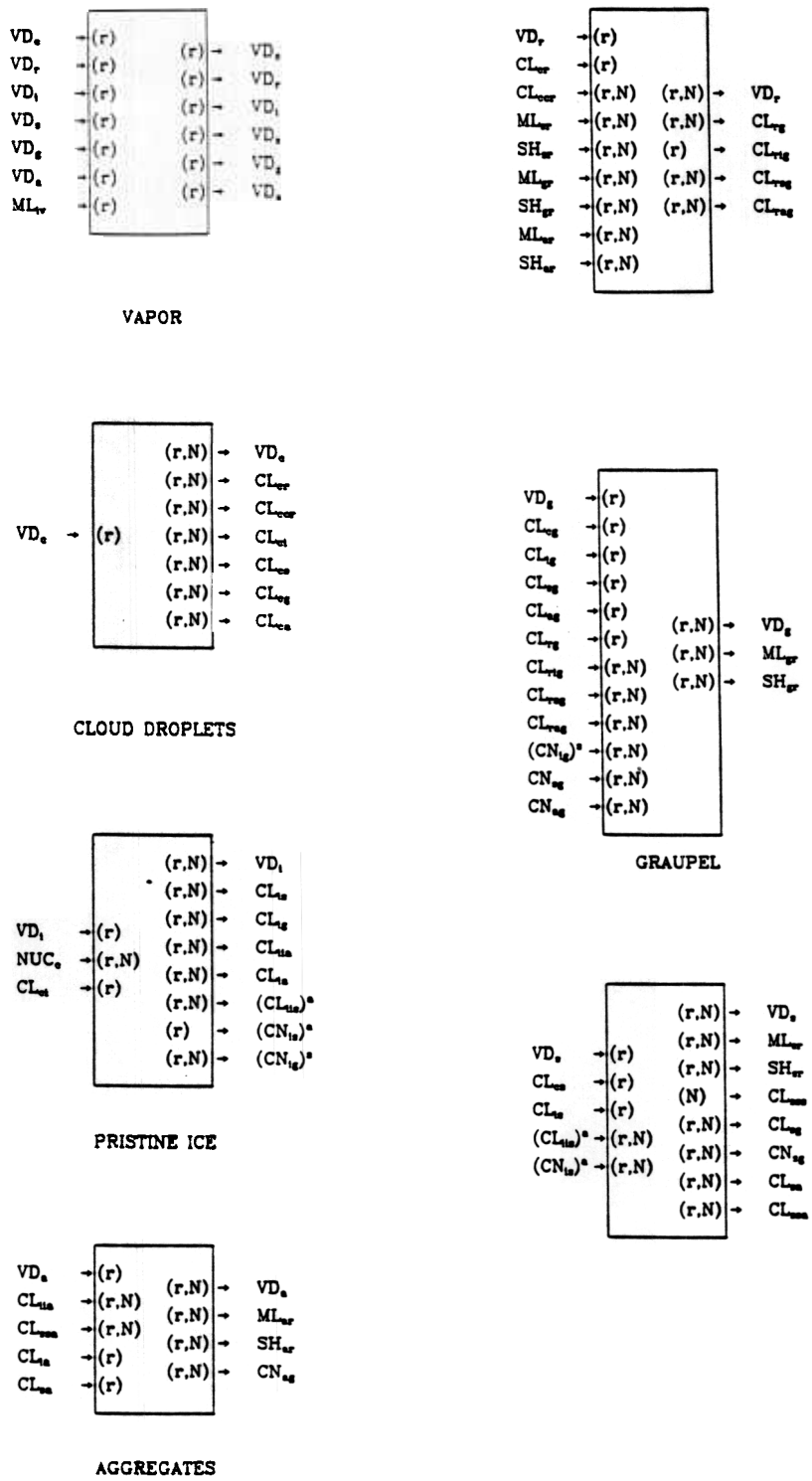

Figure 3: All possible interactions between the various categories possible in the CSU-RAMS model. The left hand side processes indicate sources, the right hand side sinks. Here VD = vapor deposition, CL = collection, CN = conversion, ML = melting, SH = shedding and NUC = nucleation. The subscripts indicate the categories involved in the process.

In this setup both the mixing ratio and the number concentration are predicted due to the nucleation, vapor deposition does not lead to a increase in the number concentration. Although the diffusional growth of pristine ice is included here, if the snow category is turned on, the mixing ratio gain due to diffusional growth is converted into the snow category, such that the pristine category experience no growth except that included in the nucleation parameterization. This results into a fixed pristine ice mean size as specified by the user in the input namelist.

- To snow: If the pristine ice category is not included in the model formulation, then the nucleation of ice needs to be included in the snow category. In that case, this is handled identical to the above discussion. If the pristine ice category is included only diffusional growth is considered, which will only impact the mixing ratio and not the number concentration.
- To graupel: Similar to the diffusional growth of rain, this can be expected to be very small. It is included for completeness and because it is routinely calculated in case the more important evaporation is occurring.
- To aggregates: Similar to rain and graupel.

2. Cloud as a source

- To vapor: This is the evaporation of cloud droplets. This can change both the number concentration and the mixing ratio of the cloud droplet population. However, since in the model the cloud droplet number concentration is a specified constant in the current formulation, in reality only the mixing ratio will be changed. With the constant number concentration this will of course lead to smaller and smaller droplets, which will all of a sudden disappear when the liquid water runs out.
- To rain: The direct conversion of cloud droplets to rain can occur by two mechanisms. First there is auto-conversion by cloud droplets forming rain, the second mechanism for moving cloud droplets to rain is collection by rain. The auto-conversion is calculated in the routine (CALCNCR) which was discussed above. This will impact the mixing ratios and the number concentration of both categories.

- To pristine ice: Although cloud droplets can convert directly to pristine ice crystals through contact nucleation, the mass transfer through this process is considered negligible in the model. Therefore, the only process considered in the model for this transfer is the collection of cloud droplets by pristine ice crystals (riming). This process does not affect the concentration of the pristine crystals, but it does that of the cloud droplet concentration. But, as with the vapor deposition on pristine ice, **if the snow category is turned on,** the mixing ratio tendency is removed from the pristine ice category and included into the snow category, such that the pristine ice crystal mixing ratio can only increase through the nucleation of pristine ice. The conversion of pristine ice to graupel due to riming will be dealt with in the section of pristine ice to graupel.
- To snow: Once again only riming is considered. This can change the mixing ratio and concentration of the cloud droplets, and the only the mixing ratio of snow. The conversion of snow to graupel due to riming will be dealt with in the section of snow to graupel.
- To graupel: Riming again, mixing ratio and concentration change for cloud droplets, only mixing ratio for graupel.
- To aggregates: Riming again, with the same consequences. However, if sufficient riming occurs, then it will covert into graupel. All the three category conversions will be treated in their steps, thus this will be considered when we discuss the conversion of aggregates to graupel.

3. Rain as a source

- To vapor: Rain is converted to vapor through evaporation (negative vapor deposition). This can lead to a concentration tendency for rain (if predicted), depending on whether the time step is long enough to completely evaporate a droplet (ie. a maximum drop size that can be evaporated totally over one timestep is calculated – then all drops smaller than that size will be removed from the distribution). This calculation is made in the vapor deposition parameterization.
- To cloud: This does not happen.

- To rain: This happens when collected rain is shed by ice hydrometeors. This does not currently impact the rain category at all, it is only mentioned here to indicate that it can happen.
- To pristine: This does not happen.
- To snow: This does not happen.
- To graupel: This can happen in two ways, first by graupel collecting rain, secondly by contact freezing of the rain droplets.

  Graupel can grow through collection of rain through the dry– or the wet growth process at subfreezing temperatures, while rain collected by graupel at temperatures above freezing will just be returned (shed) to the rain category, as will the non-frozen water from the wet growth regime. However, at this stage, all rain collected by graupel is added to the graupel category, the shedding is handled when graupel is considered as a source. This process affects both the mixing ratio and number concentration (if predicted) of the rain category.

  The second way that rain may produce graupel is through contact freezing. This can happen in two ways. If rain collides will ice at warmer subfreezing temperatures and the ice is undergoing wet growth (as evidenced by a surface temperature of 273.16 K, then some of the collected rain will freeze and some will be shed off (which can change the size distribution of the rain). At cold temperatures, contact with ice will immediately cause freezing. For simplicity it is assumed that droplets smaller than the ice particle will become rime on ice particles while droplets larger than the ice will freeze and become graupel. For this process only interactions with the remaining ice categories (pristine ice, snow and aggregates) are considered since the graupel was treated separately above. These collisions results in a reduction in mixing ratio and concentration (if predicted) of both the rain and the ice category, while it produce an increase in the graupel concentration and mixing ratio.
- To aggregates: This does not happen.

4. Pristine ice as a source.

- To vapor: Pristine crystals convert to vapor when they evaporate. It is also assumed in the model that the melting of pristine ice also converts to vapor (see next point).
- To cloud: This might actually happen for small pristine ice crystals, but it is ignored in the model. It is assumed that the melting pristine ice converts to vapor, and if this leads to a supersaturation, that the cloud water mixing ratio will increase.
- To rain: It does not happen. It is assumed that the pristine ice is to small to melt into the rain category.
- To snow: Due to different options (as far as what categories are included) that can be set in the model, there are various options here.

  First, pristine ice can be collected by snow. This process will result in a mixing ratio and concentration tendency for the pristine ice, and only in a mixing ratio tendency for the snow.

  Then, **if there is no aggregate category**, the snow category has to function as the aggregate category. The collection of pristine ice by pristine ice (aggregation) which would normally end up in the aggregate category, then end up in the snow category. *In this section it was chosen not to use the ice-autoconversion routine (CALCNIA), but rather the rates calculated in (CALCLXY) for pristine ice collecting pristine.* This process will result in mixing ratio and number concentration (if predicted) for both the snow and the pristine ice categories.

  Now, when both the pristine ice and the snow category is turned on, then the pristine ice category is not allowed to grow by either vapor deposition or riming, and these tendencies are added to the snow category. This will produce no concentration tendency for the pristine ice crystals. To calculate a number tendency for the snow crystals, it is assumed that the total of the mixing ratio tendency due to vapor deposition and riming may be converted to a number tendency based on a mass per snow crystal of 10 $\times$ the user specified minimum ice crystal mass.
- To graupel: This is accomplished through the collection if pristine ice by graupel, which results in a number and mixing ratio tendency for the pristine category, but only in a mixing ratio tendency for the graupel category. **If the snow category in not**

included in the model formulation, then the pristine category is allowed to grow through vapor deposition, but the growth through riming is converted to the graupel category. This results in a mixing ratio and number concentration tendency for both the pristine and the graupel categories, with the number concentration tendency determined from the mixing ratio tendency and a assumed mass for a single graupel particle which is equivalent to a 540 μm diameter drop.

- To aggregates: This can occur by two processes. First there is the auto-conversion of pristine ice to aggrgetes, calculated in (CALCNIA), while the second process is the collection of pristine ice by aggregates. The collection process will change the number concentration and mixing ratio of the pristine ice, and only the mixing ratio of the aggregates, while the auto-conversion process will change the mixing ratio and number concentration of both categories.

5. Snow as a source

- To vapor: Snow converts to vapor by evaporation. This will affect the mixing ratio and may affect the number concentration of the snow category.
- To cloud: This does not happen. Snow melts into the rain category.
- To rain: It is assumed that melting snow will form rain droplets. Melting of snow only occurs when the surface temperature of the snow is greater or equal to 273.16 K. If this is the case, then the cloud droplets collected as well as the vapor deposited on the snow category is assumed to be shed together with the mass melted. This results in a number concentration and mixing ratio tendency for both the rain and the snow categories. The number concentration tendency for the snow category is the sum of the tendencies calculated in the melting and collection routines, while the number of rain drops shed is based on the mixing ratio shed and a assumed rain drop diameter of 540 μm.
- To pristine ice: This does not happen in the model.
- To snow: This is calculated only if the aggregate category is not active for a simulation. This then is an implied aggregation process which will only affect the number concentration of the snow.

- To graupel: Snow converts to graupel through the collection of it by the graupel. This results in a concentration and mixing ratio tendency for the snow, and only a mixing ratio tendency for the graupel. Heavily rimed snow will also convert to graupel. The philosophy used here is to transfer the amount of rime in excess of the deposition and ice crystal collection rates. The physical reasoning is that when riming dominates growth, then there will be a rapid conversion to graupel. Once the mixing ratio tendency has been determined, a number concentration tendency has to be determined. The average snow mass is calculated based on the power law coefficients for the snow category defined in Table 8 and the mean snow diameter. It is assumed that the rimed snow crystals will be bigger than the average snow crystal, so that the average mass of the converted crystals is twice that of the average snow crystal. This concentration change will be the same for the snow and the graupel categories.
- To aggregates: Snow can convert to aggregates due to collection of snow by aggregates or through the autoconversion of snow (calculated in (CALCNIA)). The first process impacts the number concentration and mixing ratio of the snow category, and only the mixing ratio of the aggregate category, while the autoconversion process impacts the number concentration and mixing ratio of both categories.

6. Graupel as a source

- To vapor: Graupel can convert to vapor by evaporation. This will result in a mixing ratio tendency, and may also result in a concentration tendency.
- To cloud: This does not happen in the model.
- To rain: Graupel can convert to rain through melting or through the shedding of water during wet growth at sub-freezing temperatures. (Currently wet-growth is not implemented in the model – there is an if statement that will calculate this conversion only at temps warmer than freezing, nothing is done at temps colder than freezing). The sum of the diffusional growth/evaporation, the collection of cloud droplets and the collection of rain is computed, and the amount of ice frozen/molten is included. The difference is then shed into the rain category. The number concentration tendency for the graupel is based on the amount of graupel molten, while the number of raindrops shed includes

the number of molten graupel as well as a number calculated from the accreted cloud water and a drop of diameter 540 μm.

- To pristine ice: This does not happen in the model.
- To snow: This does not happen in the model.
- To aggregates: This does not happen in the model.

7. Aggregates as a source

- To vapor: Aggregates convert to vapor when they evaporate. This results in a mixing ratio tendency, and may also result in a number concentration tendency.
- To rain: It is assumed that melting aggregates have sufficient mass to be classified as rain. Once again, this will only be computed when the surface temperature of the aggregates are at or warmer than freezing. The sum of the diffusional growth/evaporation and the collection of cloud droplets is computed, then the amount of ice frozen/molten is included, and the amount of aggregates collected by rain at environmental temperatures greater the freezing is added. Of course, at temperatures below freezing, the collection of aggregates by rain results in graupel. For the number concentration tendency of the aggregate category, it is assumed that the number of aggregates molten and the number of aggregates collected by rain at warmer than freezing temperatures contribute, while the number concentration tendency for the rain category is made up of the number of aggregates molten plus the number of 540 μm diameter droplets making up the amount of mass added to the aggregate category due to diffusional growth/evaporation and the collection of cloud droplets.
- To pristine: This does not happen in the model.
- To snow: This does not happen in the model.
- To graupel: The same philosophy is used here as in the snow conversion to graupel. First, aggregates can convert to graupel through the collection of it by graupel. This results in a concentration and mixing ratio tendency for the aggregate category, but only a mixing ratio tendency for the graupel category. Secondly, at sub-freezing temperatures, the amount of rime (cloud and rain) in excess of the deposition and ice crystal collection

rates is transferred to the graupel category. The average aggregate mass is calculated, and it is assumed that the average rimed aggregate converting to graupel is twice the mass of the average aggregate. This concentration change will be the same for the aggregate and the graupel categories.

This is the end of the conversion subroutine. It is possible that over the course of a time step, that the calculated conversions may completely consume a category, or even produce a negative mixing

This, of course, is not physical, and is prevented such that the maximum amount of any category that may be consumed is the amount that is available.

6.5.6 Repairs to conversions

In the flow of the program as we have been following it, the call to (REPAIR) is the last call from the driver routine (MTEND). This routine checks all computed conversions to see if they will cause a quantity to become negative over the course of a time step. If so, the losses are reduced. If this is required, this is the point were the program departs from its physical base. The tendencies for the category that obtain negative mixing ratio values (concentration currently is not checked) are reduced on a percentage basis to give a zero mixing ratio at the end of the time step. However, since the loss of one category is a gain for another category, everything is interrelated, and therefore this is done as a iterative process which will continue until all the categories remain positive definite. The repair is done with some physical insight: For instance, vapor deposition cannot reduce the vapor mixing ratio below saturation, while the Bergeron-Findeisen process allows the cloud water to be an instantaneous source for vapor. At the end of this routine, the control is returned to (MTEND) and then from (MTEND) back to (MICPHYS), the top level microphysical driver subroutine.

Calculation of the final tendencies

The last call from (MICPHYS) is made to (MDLTEND), another driver subroutine which then calculates the mixing ratio and number concentration tendencies required by the model. The routine (CALTEND) is called from (MDLTEND) for each category turned on in the model, and finally the vapor mixing ratio is calculated in (MDLTEND) itself.

Since each category in (MTEND) was considered only as a source to the other categories, the final mixing ratio tendency for any category has to be constructed by the addition of all the conversions

of all categories towards this category, minus the sum of all the conversions from this category to all the others.

The number concentration tendency for each category is constructed by adding the number concentrations produced (3 in the second dimension of the CNVSN array) for a category and subtracting the numbers lost (2 in the second dimension of the CNVSN array) for that category. (The comments in the code say that this is converted into a log tendency, but there is no evidence in the code.

This completes one run through the microphysical package.

Part IV
CONSERVATION EQUATIONS

7 In the dynamic model

The microphysical package only calculates the various sources and sinks of all the microphysical categories, and it does not address advection, precipitation or turbulent effects. To describe the above dynamic processes fall beyond the scope of this paper, but we will list all the relevent equations. In this discussion a quick overview of the routine (THERMO) of the dynamic model will be given. To do this, it is necessary to define two variables used by the model, the Exner function π

$$\pi = c_p \left(\frac{P}{P_{00}} \right)^{R/c_p} \tag{7.1}$$

and the ice-liquid water potential temperature (Tripoli and Cotton, 1981) θ_{il}

$$\theta = \theta_{il} \left(1 + \frac{L_{vl} r_{liq} + L_{iv} r_{ice}}{c_p \max(T, 253)} \right) \tag{7.2}$$

where c_p is the specific heat capasity for dry air at constant pressure, P is the total ambient pressure, P_{00} = 1000 hPa, R is the gas constant for dry air, L_{vl} is the latent heat of condensation, L_{iv} is the latent heat of sublimation, and T and θ are the temperature and the potential temperature respectively. The quantities r_{liq} and r_{ice} are the total liquid water and ice water mixing ratios respectively.

The Exner function, the total pressure, the dry potential temperature and the mixing ratio is first calculated. Then the saturation mixing ratio is calculated and it determined whether or not there is any condensate or supersaturation at any gridpoint. Gridpoints with condensate are gathered into one dimensional vectors for the optimization of code on vector computors. The mixing ratios of water vapor and cloud droplets are diagnosed from the total water mixing ratio (r_T), which is a model variable, in the following way. First the total liquid water mixing ratio (r_{liq}) is calculated as

$$r_{liq} = r_c + r_r \tag{7.3}$$

If any of the ice categories has been activated, the total ice water mixing ratio (r_{ice}) is calculated as

$$r_{ice} = r_i + r_s + r_a + r_g$$

The cloud droplet mixing ratio (r_c) and the water vapor mixing ratio (r_v) are diagnosed from (r_T), (r_{liq}) and (r_{ice}) by using the saturation mixing ratio (r_{vs}) over water.

$$r_v = \max(0, r_T - r_{liq} - r_{ice})$$

and

$$r_c = \max(0, r_T - r_{liq} - r_{ice} - r_{vs})$$

This set of equations can be solved iteratively to produce a diagnosis of T, θ, r_{vs}, r_v, and r_c from predictions of θ_{il}, π, r_T, r_i, r_s, r_a, r_g, and r_r.

To force complete freezing at a specified homogenous nucleation temperature (T_H), the above set of equations is changed as follows (for $T < T_H$):

$$r_c = 0$$

$$r_r^* = 0$$

$$r_i^* = r_i + r_r + \max(r_T - r_{vs} - r_{ice}, 0)$$

where the asterisk means temporary values during iteration. After iteration the permanent values of r_r and r_i are altered to the temporary values.

With the mixing ratios of cloud droplets and water vapor now diagnosed, the microphysics module is called. The microphysics package calculates the mixing ratio and concentration tendency due to the sources and sinks, as well as the mass-weighted mean terminal velocity for each category. These values are used in the conservation equations for rain, pristine ice, snow, aggregates and graupel.

Upon completion of the above calculations, the one dimensional vectors are scattered back into three dimension space, and the precipitation tendencies are calculated. At this stage, all the terms in the conservation equations have been calculated, and the microphysical tendencies are calculated from the following set of equations.

The following notation conventions will be used in this section, first, the operators:

ADV(A)	is the advection operator, defined elsewhere
TURB(A)	is the turbulence operator, also defined elsewhere
CL_{ab}	is the collection of category a by category b
VD_a	is vapor deposition/evaporation on category a
NUC_a	is nucleation of category a
ML_a	is the melting of category a

We will also make extensive use of delta functions, which we modified to operate on temperature criteria. The subscripts of the delta functions will identify the temperature regimes where it is effective, i.e.

$$\delta_{T<} = \begin{cases} 1 & \text{if } T < 273.16 \text{ K where } T \text{ is the temperature} \\ 0 & \text{otherwise} \end{cases}$$

The condition may be on the temperature of the air (T) or the surface temperature of a particle (T_s), and it will be conditioned on whether this temperature is equal, greater, greater or equal, etc., that the freezing temperature 273.16 K.

The following subscripts are used:

v	for vapor
c	for cloud droplets
r	for rain
i	for pristine ice
s	for snow
a	for aggregates
g	for graupel

The conservation equations will be written in three parts, the advection terms, the sinks and lastly the sources. Subscripts indicate the categories involved – a double subcript indicate a conversion from subscript one to subscript two, a triple subscript indicates interaction between subscripts one and two that convert to subscript 3. Superscripts indicates interactions that will only be considered if that category is not included.

Water vapor – although it is diagnosed in the model, there are implied sources and sinks:

$$\frac{\partial}{\partial t}(\rho_0 r_v) = \text{ADV}(\rho_0 r_v) + \rho_0 \text{TURB}(r_v)$$

$$-\rho_0 [VD_c + VD_r + \delta_{T<}(NUC_i + \max(0, VD_i))_{vi}$$

$$+ VD_s + VD_a + VD_g]$$

$$+\rho_0[\max(0, -VD_i)_{iv}]$$

Cloud water – although it is diagnosed in the model, there are implied sources and sinks:

$$\frac{\partial}{\partial t}(\rho_0 r_c) = \text{ADV}(\rho_0 r_c) + \rho_0 \text{TURB}(r_c) - \frac{1}{\rho_0}\frac{\partial}{\partial z}(\rho_0 v_c r_c)$$

$$-\rho_0 [CL_{ccr} + \delta_{T<}(CL_{ci}) + CL_{cs} + CL_{ca} + CL_{cg}]$$

$$+\rho_0 [VD_c]$$

Rain:

$$\frac{\partial}{\partial t}(\rho_0 r_r) = \text{ADV}(\rho_0 r_r) + \rho_0 \text{TURB}(r_r) - \frac{1}{\rho_0}\frac{\partial}{\partial z}(\rho_0 v_g r_r)$$

$$-\rho_0 [CL_{rg} + \delta_{T<}(CL_{ri} + CL_{rs} + CL_{ra})_{rg}]$$

$$\begin{aligned}
&+\rho_0 [\, VD_r + CL_{ccr} \\
&\quad + \delta_{T_s\geq}\{\max(0, VD_s + CL_{cs} + ML_s) + \delta_{T\geq}(CL_{sr})\}_{sr} \\
&\quad + \delta_{T_s\geq}\{\max(0, VD_g + CL_{cg} + CL_{rg} + \delta_{T<}(CL_{ri} + CL_{rs} + CL_{ra}) + ML_g)\}_{gr} \\
&\quad + \delta_{T_s\geq}\{\max(0, VD_a + CL_{ca} + ML_a) + \delta_{T\geq}(CL_{ar})\}_{ar}\,]
\end{aligned}$$

Pristine ice:

$$\frac{\partial}{\partial t}(\rho_0 r_i) = \text{ADV}(\rho_0 r_i) + \rho_0 \text{TURB}(r_i) - \frac{1}{\rho_0}\frac{\partial}{\partial z}(\rho_0 v_i r_i)$$

$$-\rho_0 [\max(0, -VD_i)_{iv} + \delta_{T<}(CL_{ci} + \max(0, VD_i))_{is}$$

$$+ CL_{ig} + [2CL_{ii}]^{a}_{is} + [\delta_{T<}(CL_{ci})]^{s}_{ig} + CL_{is} + CL_{ia} + CL_{iia} \,]$$

$$+\rho_0 \,[\delta_{T<}(NUC_i + \max(0, VD_i))_{vi} + \delta_{T<}(CL_{ci})]$$

Snow:

$$\frac{\partial}{\partial t}(\rho_0 r_s) = \text{ADV}\,(\rho_0 r_s) + \rho_0 \text{TURB}(r_s) - \frac{1}{\rho_0}\frac{\partial}{\partial z}(\rho_0 v_s r_s)$$

$$-\rho_0 \,[\, \delta_{T_s\geq}\{\max(0, VD_s + CL_{cs} + ML_s) + \delta_{T\geq}(CL_{sr})\}_{sr}$$
$$+ \max(0, \delta_{T_s=}\{\max(0, -ML_s)\} + \delta_{T_s<}\{CL_{cs} + CL_{rs}\} - VD_s - CL_{is} - CL_{as})_{sg}$$
$$+ CL_{sg} + CL_{ssa} + CL_{sa} \,]$$

$$+\rho_0 \,[\, VD_s + CL_{cs} + CL_{is} + [2CL_{ii}]^{a}_{is}$$
$$+ \delta_{T<}(CL_{ci} + \max(0, VD_i))_{is} \,]$$

Graupel:

$$\frac{\partial}{\partial t}(\rho_0 r_g) = \text{ADV}\,(\rho_0 r_g) + \rho_0 \text{TURB}(r_g) - \frac{1}{\rho_0}\frac{\partial}{\partial z}(\rho_0 v_g r_g)$$

$$-\rho_0 \,[\delta_{T_s\geq}\{\max(0, VD_g + CL_{cg} + CL_{rg} + \delta_{T<}(CL_{ri} + CL_{rs} + CL_{ra}) + ML_g)\}_{gr}]$$

$$+\rho_0 \,[\, VD_g + \delta_{T<}(CL_{ri} + CL_{rs} + CL_{ra})_{rg}$$
$$+ CL_{cg} + CL_{rg} + CL_{ig} + CL_{sg} + CL_{ag}$$
$$+ \max(0, \delta_{T_s=}\{\max(0, -ML_s)\} + \delta_{T_s<}\{CL_{cs} + CL_{rs}\} - VD_s - CL_{is} - CL_{as})_{sg}$$
$$+ \max(0, \delta_{T_s=}\{\max(0, -ML_a)\} + \delta_{T_s<}\{CL_{ca} + CL_{ra}\} - VD_a - CL_{ia} - CL_{sa})_{ag}$$
$$+ [\delta_{T<}(CL_{ci})]^{s}_{ig} \,]$$

Aggregates:

$$\frac{\partial}{\partial t}(\rho_0 r_a) = \mathrm{ADV}(\rho_0 r_a) + \rho_0 \mathrm{TURB}(r_a) - \frac{1}{\rho_0}\frac{\partial}{\partial z}(\rho_0 v_g r_a)$$

$$-\rho_0 [\, \delta_{T_s \geq}\{\max(0, VD_a + CL_{ca} + ML_a) + \delta_{T \geq}(CL_{ar})\}_{ar}$$
$$+ \max(0, \delta_{T_s =}\{\max(0, -ML_a)\} + \delta_{T_s <}\{CL_{ca} + CL_{ra}\} - VD_a - CL_{ia} - CL_{sa})_{ag}$$
$$+ CL_{ag}\,]$$

$$+\rho_0 [VD_a + CL_{ca} + CL_{ia} + CL_{sa} + CL_{iia} + CL_{ssa}]$$

Part V
APPENDICES

A The gamma function

The gamma function is defined by the following formulas (taken from Gradshteyn and Ryzhik, 1980 and Abramowitz and Stegun, 1964):

$$\Gamma(x) = \int_0^\infty e^{-t} t^{x-1} dt \quad [\mathrm{Re}\, x > 0]$$

$$\Gamma(x+1) = x\Gamma(x)$$

$$\Gamma(nx) = (2\pi)^{\frac{1-n}{2}} n^{nx-\frac{1}{2}} \prod_{k=0}^{n-1} \Gamma\left(x + \frac{k}{n}\right) \quad \text{[product theorem]}$$

$$\Gamma(2x) = \frac{2^{2x-1}}{\sqrt{\pi}} \Gamma(x)\Gamma\left(x + \frac{1}{2}\right) \quad \text{[doubling formula]}$$

A few particular values of the gamma function are:

$$\Gamma(1) = \Gamma(2) = 1.$$

$$\Gamma(\tfrac{1}{2}) = \sqrt{\pi}.$$

$$\Gamma\left(-\frac{1}{2}\right) = -2\sqrt{\pi}.$$

and for n a natural number:

$$\Gamma(n) = (n-1)!$$

$$\Gamma(n + \tfrac{1}{2}) = \frac{\sqrt{\pi}}{2^n}(2n-1)!$$

$$\Gamma(\tfrac{1}{2} - n) = (-1)^n \frac{2^n \sqrt{\pi}}{(2n-1)!}$$

As a quick lookup guide for the use of the gamma function, the values of $\Gamma(x)$ has been tabulated for $1.0 < x < 6.9$ in Table 9.

B Incomplete gamma function

Next the basic formulas defining the two incomplete gamma functions $\gamma(\alpha, x)$ and $\Gamma(\alpha, x)$ are given.

$$\gamma(\alpha, x) = \int_0^x e^{-t} t^{\alpha-1} dt \quad [\mathrm{Re}\, \alpha > 0]$$

$$\Gamma(\alpha, x) = \int_x^\infty e^{-t} t^{\alpha-1} dt \tag{B.1}$$

x	$\Gamma(x)$	x	$\Gamma(x)$	x	$\Gamma(x)$
1.0	1.00	3.00	2.00	5.00	24.00
1.1	0.95	3.10	2.20	5.10	27.93
1.2	0.92	3.20	2.42	5.20	32.58
1.3	0.90	3.30	2.68	5.30	38.08
1.4	0.89	3.40	2.98	5.40	44.60
1.5	0.89	3.50	3.32	5.50	52.34
1.6	0.89	3.60	3.72	5.60	61.55
1.7	0.91	3.70	4.17	5.70	72.53
1.8	0.93	3.80	4.69	5.80	85.62
1.9	0.96	3.90	5.30	5.90	101.27
2.0	1.00	4.00	6.00	6.00	120.00
2.1	1.05	4.10	6.81	6.10	142.45
2.2	1.10	4.20	7.76	6.20	169.41
2.3	1.17	4.30	8.86	6.30	201.81
2.4	1.24	4.40	10.14	6.40	240.83
2.5	1.33	4.50	11.63	6.50	287.89
2.6	1.43	4.60	13.38	6.60	344.70
2.7	1.54	4.70	15.43	6.70	413.41
2.8	1.68	4.80	17.84	6.80	496.61
2.9	1.83	4.90	20.67	6.90	597.49

Table 9: Tabulation of complete gamma function for $1.0 < x < 6.9$

Some special cases are also defined:

$$\gamma(1+n,x) = n!\left[1 - e^{-x}\left(\sum_{m=0}^{n}\frac{x^m}{m!}\right)\right] \quad [n = 0,1,\ldots]$$

$$\Gamma(1+n,x) = n!e^{-x}\sum_{m=0}^{n}\frac{x^m}{m!} \quad [n = 0,1,\ldots] \tag{B.2}$$

The incomplete gamma functions may generally also be approximated in a series representation given by

$$\gamma(\alpha,x) = \Gamma(\alpha)x^{\alpha}e^{-x}\sum_{n=0}^{\infty}\frac{x^n}{\Gamma(\alpha+n+1)} = \sum_{n=0}^{\infty}\frac{(-1)^n x^{\alpha+n}}{\Gamma(n+1)(\alpha+n)}$$

$$\Gamma(\alpha,x) = \Gamma(\alpha) - \sum_{n=0}^{\infty}\frac{(-1)^n x^{\alpha+n}}{n!(\alpha+n)} \quad [\alpha \neq 0,-1,-2,\ldots] \tag{B.3}$$

Some functional relationships involving the incomplete gamma functions are given by

$$\gamma(\alpha+1,x) = \alpha\gamma(\alpha,x) - x^{\alpha}e^{-x}$$

$$\Gamma(\alpha+1,x) = \alpha\Gamma(\alpha,x) + x^{\alpha}e^{-x}$$

$$\Gamma(\alpha,x) + \gamma(\alpha,x) = \Gamma(\alpha)$$

$$\frac{d\gamma(\alpha,x)}{dx} = -\frac{d\Gamma(\alpha,x)}{dx} = x^{\alpha-1}e^{-x}$$

C Integrals often used in microphysics parameterization

In this section some standard forms of integrals that are often used in microphysical parameterization are listed. These integrals were taken from Gradshteyn and Ryshik (1980)

$$\int_0^u x^n e^{-\mu x}dx = \frac{n!}{\mu^{n+1}} - e^{-u\mu}\sum_{k=0}^{n}\frac{n!}{k!}\frac{u^k}{\mu^{n-k+1}} \quad [u>0,\ \mathrm{Re}\,\mu>0]$$

$$\int_u^\infty x^n e^{-\mu x}dx = e^{-u\mu}\sum_{k=0}^{n}\frac{n!}{k!}\frac{u^k}{\mu^{n-k+1}} \quad [u>0,\ \mathrm{Re}\,\mu>0]$$

$$\int_0^\infty x^n e^{-\mu x} = n!\mu^{-n-1} \quad [\mathrm{Re}\,\mu>0]$$

$$\int_0^u x^{\nu-1}e^{-\mu x}dx = \mu^{-\nu}\gamma(\nu,\mu u) \quad [\mathrm{Re}\,0]$$

$$\int_0^u x^{p-1}e^{-x}dx = \sum_{k=0}^{\infty}(-1)^k\frac{u^{p+k}}{k!(p+k)}$$

$$\int_0^u x^{p-1}e^{-x}dx = e^{-u}\sum_{k=0}^{\infty}\frac{u^{p+k}}{p(p+1)\ldots(p+k)}$$

$$\int_u^\infty x^{\nu-1}e^{-\mu x}dx = \mu^{-\nu}\Gamma(\nu,\mu u) \quad [u>0,\ \mathrm{Re}\,\mu>0]$$

$$\int_0^\infty x^{\nu-1}e^{-\mu x} = \frac{1}{\mu^\nu}\Gamma(\nu) \quad [\mathrm{Re}\,\mu>0,\ \mathrm{Re}\,\nu>0]$$

$$\int_{-\infty}^{\infty}\exp(-p^2x^2 \pm qx)dx = \exp\left(\frac{q^2}{4p^2}\right)\frac{\sqrt{\pi}}{p} \quad [p>0]$$

$$\int_0^\infty x^{\mu-1}e^{-\beta x}\Gamma(\nu,\alpha x)dx = \frac{\alpha^\nu\Gamma(\mu+\nu)}{\mu(\alpha+\beta)^{\mu+\nu}}\,{}_2F_1\left(1,\mu+\nu;\mu+1;\frac{\beta}{\alpha+\beta}\right)$$
$$[\mathrm{Re}\,(\alpha+\beta)>0,\ \mathrm{Re}\,\mu>0,\ \mathrm{Re}\,(\mu+\nu)>0]$$

$$\int_0^\infty x^{\mu-1}e^{-\beta x}\Gamma(\nu,\alpha x)dx = \frac{\alpha^\nu\gamma(\mu+\nu)}{\mu(\alpha+\beta)^{\mu+\nu}}\,{}_2F_1\left(1,\mu+\nu;\nu+1;\frac{\alpha}{\alpha+\beta}\right)$$
$$[\mathrm{Re}\,(\alpha+\beta)>0,\ \mathrm{Re}\,\beta>0,\ \mathrm{Re}\,(\mu+\nu)>0] \qquad (C.4)$$

where ${}_2F_1$ is the Gauss hypergeometric series.

D Collection integrals

To calculate collection terms we need integral of the form

$$I = \int_0^\infty x^{\mu-1} e^{-\beta x} \gamma(\nu, \alpha x) dx \tag{D.1}$$

Using (B.3) we have

$$I = \Gamma(\nu)\alpha^\nu \sum_{n=0}^{\infty} \int_0^\infty \frac{e^{-(\alpha+\beta)x} x^{\mu+\nu+n-1}}{\Gamma(\nu+n+1)} dx \tag{D.2}$$

Integration of each term of the sum gives

$$I = \frac{\Gamma(\nu)\alpha^\nu}{(\alpha+\beta)^{\mu+\nu}} \sum_{n=0}^{\infty} \left(\frac{\alpha}{\alpha+\beta}\right)^n \frac{\Gamma(\nu+\mu+n)}{\Gamma(\nu+n+1)} \tag{D.3}$$

We found this series suitable for calculations in some cases but for large n the Γ functions becomes excessively large leading to numerical difficulties. Thus we reexpressed (D.3) in terms of complete beta function defined as

$$B(x,y) = \frac{\Gamma(x)\Gamma(y)}{\Gamma(x+y)} \tag{D.4}$$

The ratio of gamma functions in (D.3) become

$$\frac{\Gamma(\nu+\mu+n)}{\Gamma(\nu+1+n)} = \frac{\Gamma(\nu+\mu)}{\Gamma(\nu+1)} \frac{B(\nu+1,n)}{B(\nu+\mu,n)} \tag{D.5}$$

and

$$I = \frac{\alpha^\nu}{\nu(\alpha+\beta)^{\mu+\nu}} \Gamma(\mu+\nu) \sum_{n=0}^{\infty} \left(\frac{\alpha}{\alpha+\beta}\right)^n \frac{B(\nu+1,n)}{B(\nu+\mu,n)}$$

Using the second form of the series representation of incomplete gamma function (B.3) we have

$$I = \sum_{n=0}^{\infty} \int_0^\infty x^{\mu-1} e^{-\beta x} \frac{(-1)^n (\alpha x)^{\nu+n}}{\Gamma(n+1)(\nu+n)} dx \tag{D.7}$$

or, integrating

$$I = \frac{\alpha^\nu}{\beta^{\mu+\nu}} \sum_{n=0}^{\infty} \left(\frac{\alpha}{\beta}\right)^n \frac{(-1)^n}{\nu+n} \frac{\Gamma(\mu+\nu+n)}{\Gamma(n+1)}$$

and using beta function we get

$$I = \frac{\alpha^\nu \Gamma(\mu+\nu)}{\beta^{\mu+\nu}} \sum_{n=0}^{\infty} \left(\frac{\alpha}{\beta}\right)^n \frac{(-1)^n}{\nu+n} \frac{B(1,n)}{B(\mu+\nu,n)}$$

Representation (D.8) and (D.9) is convergent for $\alpha < \beta$, thus it is less suitable for calculations than (D.3) and (D.6). We found (D.6) to have good numerical behavior.

We were not able to integrate in closed form the more general case of

$$I = \int_0^\infty x^{\mu-1} e^{-\beta x} \gamma(\nu, \alpha x^p) dx \tag{D.10}$$

This integral was evaluated numerically using QAGI routine from the QUADPACK package (available in SLATEC, IMSL or NETLIB libraries).

References

Abramowitz, M. and I. A. Stegun, 1964: *Handbook of mathematical functions with formulas, graphs and mathematical tables.* Dover.

Alofs, D. J. and T. Lui, 1981: Atmospheric measurements of ccn in the supersaturation range 0.013–0.681%. *J. Atmos. Sci.*, **38**, 2772—2778.

Beard, K. V. and H. R. Pruppacher, 1971: A wind tunnel investigation of the rate of evaporation of small water drops falling at terminal velocity in air. *J. Atmos. Sci.*, **28**, 1455—1464.

Berezinskiy, N. A. and G. V. Stepanov, 1986: Dependence of the concentration of natural ice-forming nuclei of different size on the temperature and supersaturation. *Izvestiya, Atmospheric and Oceanic Physics*, **22**, 722—727.

Berry, E. X. and R. L. Reinhardt, 1974: Analysis of cloud drop growth by collection: Part IV. a new parameterization. *J. Atmos. Sci.*, **31**, 2127—2135.

Berry, E. X. and R. L. Reinhardt, 1974: Analysis of cloud drop growth by collection: Part III. Accretion and self-collection. *J. Atmos. Sci.*, **31**, 2118—2126.

Berry, E. X. and R. L. Reinhardt, 1974: Analysis of cloud drop growth by collection: Part II. Single initial distributions. *J. Atmos. Sci.*, **31**, 1825—1831.

Berry, E. X. and R. L. Reinhardt, 1974: Analysis of cloud drop growth by collection: Part I. Double distributions. *J. Atmos. Sci.*, **31**, 1814—1824.

Byers, H. R., 1965: *Elements of cloud physics.* University of Chicago Press, Chicago.

Clark, T. L. and W. D. Hall, 1983: A cloud physical parameterization method using movable basis functions: stochastic coalescence parcel calculations. *J. Atmos. Sci.*, **40**, 1709—1728.

Cotton, W. R. and R. Anthes, 1989: *Storm and Cloud Dynamics.* Academic Press, Inc. 828 pp.

Cotton, W. R., M. A. Stephens, T. Nehrkorn, and G. J. Tripoli, 1982: The Colorado State University three-dimensional cloud/mesoscale model - 1982, Part II: an ice parameterization. *J. Rech. Atmos.*, **16**, 295—320.

Cotton, W. R., G. Tripoli, R. M. Rauber, and E. A. Mulvihill, 1986: Numerical simulation of the effects of varying ice crystal nucleation rates and aggregation processes on orographic snowfall. *J. Climate Appl. Meteor.*, **25**, 1658—1680.

Derickson, R. G. and W. R. Cotton, 1977: *On the use of finite Taylor's series approximations to certain exponential and power functions employed in cloud models.* Technical Report, Dept. Atmos. Sci., Colo. State Univ., Ft Collins, Co 80523.

Feingold, G. and Z. Levin, 1986: The lognormal fit to raindrop spectra from frontal convective clouds in Israel. *J. Clim. Appl. Meteor.*, **25**, 1346—1363.

Fletcher, N. H., 1962: *Physics of rain clouds.* Cambridge University Press. 386 pp.

Foote, G. B. and P. S. du Toit, 1969: Terminal velocity of raindrops aloft. *J. Appl. Meteor.*, **8**, 249—253.

Gordon, G. L. and J. D. Marwitz, 1981: Secondary ice crystal production in stable orographic clouds over the sierra nevada. In *Eighth Conf. on Inadvertent and Planned Weather Modification*, pages 62—63, Amer. Meteor. Soc.

Gordon, G. L. and J. D. Marwitz, 1984: An airborne comparison of three PMS probes. *J. Atmos. Ocean. Tech.*, **1**, 22—27.

Gradshteyn, I. S. and I. M. Ryzhik, 1980: *Table of integrals, series, and products.* Academic Press, Inc.

Hallet, J. and S. C. Mossop, 1974: Production of secondary ice particles during the riming process. *Nature*, **249**, 26—28.

Hallgren, R. E. and C. L. Hosler, 1960: Preliminary results on the aggregation of ice crystals. *Geophys. Monogr. Am. Geophys. Union*, **5**, 257—263.

Heymsfield, A. J., 1972: Ice crystal terminal velocities. *J. Atmos. Sci.*, **29**, 1348—1356.

Hobbs, P. V. e. a., 1972: *Contributions from the cloud physics group, Research report VII. Dept. Atmos. Sci.* Technical Report, Univ. of Washington, Seattle, Wash. 293pp.

Hosler, C. L. and R. E. Hallgren, 1960: The aggregation of small ice crystals. *Discuss. Faraday Soc.*, **30**, 200—208.

Huffman, P. J. and G. Vali, 1973: The effect of vapor depletion on ice nucleus measurements with membrane filters. *J. Appl. Meteor.*, **12**, 1018—1024.

Jiusto, J. E., 1967: Aerosol and cloud microphysics measurements in Hawaii. *Tellus*, **19**, 359—368.

Kessler, E., 1969: . *On the distribution and continuity of water substance in atmospheric circulations.* Meteor. Monogr., No 32, Amer. Meteor. Soc., 84 pp.

Kochmond, W. C., 1965: . *Investigation of warm fog properties and fog modification concepts.* 2nd Ann. Rep., Res Dept. RM-1788-P-9, pp36—47. Cornell Earonaut. Lab., Buffalo, N.Y.

Latham, J. and C. P. R. Saunders, 1971: Experimental measurements of the collection efficiencies of ice crystals in electric fields. *Quart. J. Roy. Meteor. Soc.*, **96**, 257—265.

Lin, Y., R. D. Farley, and H. D. Orville, 1983: Bulk parameterization of the snow field in a cloud model. *J. Atmos. Sci*, **22**, 1065—1089.

List, R., editor, 1968: *Smithsonian Meteorological Tables.* Volume 114, Smithsonian Inst. Press, City of Washington.

Locatelli, J. D. and P. V. Hobbs, 1974: Fallspeeds and masses of solid precipitation particles. *J. Geophys. Res.*, **79**, 2185—2197.

Ludlam, F. H., 1980: *Clouds and storms: The behavior and effect of water in the atmosphere.* Penn. State Univ. Press.

Magono, C. and T. Nakamura, 1965: Aerodynamic studies of falling snow flakes. *J. Meteor. Soc. Japan*, **43**, 139—147.

Manton, M. J. and W. R. Cotton, 1977: Parameterization of the atmospheric surface layer. *J. Atmos. Sci.*, **34**, 331—334.

Mossop, S. C., 1976: Production of secondary ice particles during the growth of graupel by riming. *Quart. J. Roy. Meteor. Soc.*, **102**, 25—44.

Passarelli, R. E. and R. C. Srivastava, 1979: A new aspect of snowflake aggregation theory. *J. Atmos. Sci.*, **36**, 484—493.

Pruppacher, H. R. and J. D. Klett, 1978: *Microphysics of clouds and precipitation.* D. Reidel Publishing Comp.

Rogers, D. C., 1973: *The aggregation of natural ice crystals.* Master's thesis, University of Wyoming, Dept. of Atmospheric Resources. 86 pp.

Rogers, R. R., 1979: *A short course in cloud physics.* Pergamon Press, Oxford.

Ryan, B. F., S. N. Wishart, and D. E. Shaw, 1976: The growth rates and densities of ice crystals between –3°c and –21°c. *J. Atmos. Sci.*, **33**, 842—851.

Scott, W. T. and C. Y. Chen, 1970: Approximate formulas fitted to the Davis-Sartor-Schafrir-Neiburger droplet collision efficiency calculations. *J. Atmos. Sci.*, **27**, 698—700.

Slinn, W. G. N. and J. M. Hales, 1971: A reevaluation of the role of thermophoresis as a mechanism of in– and below–cloud scavenging. *J. Atmos. Sci.*, **28**, 1465—1471.

Tripoli, G. J. and W. R. Cotton, 1980: A numerical investigation of several factors contributing to the observed variable intensity of deep convection over South Florida. *J. Appl. Meteor.*, **19**, 1037—1063.

Tripoli, G. J. and W. R. Cotton, 1981: The use of ice-liquid water potential temperature as a thermodynamic variable in deep atmospheric models. *Mon. Wea. Rev.*, **109**, 1094—1102.

Twomey, S., 1959: The nuclei of natural cloud formation, Part II: The supersaturation in natural clouds and the variation of cloud droplet concentration. *Geofys. Pura E Appl.*, **43**, 243—249.

Twomey, S. and T. A. Wojciechowski, 1969: Observations of geophysical variation of cloud nuclei. *J. Atmos. Sci.*, **26**, 684—688.

Young, K. C., 1974: A numerical simulation of wintertime, orographic precipitation. I: Description of model microphysics and numerical techniques. *J. Atmos. Sci.*, **31**, 1735—1748.

Young, K. C., 1974: The role of contact nucleation in ice phase initiation in clouds. *J. Atmos. Sci.*, **31**, 768—776.

Ziegler, C. L., 1985: Retrieval of thermal and microphysical variables in observed convective storms. Part I: model development and preliminary testing. *J. Atmos. Sci.*, **42**, 1487—1509.